

MATERIALS PATTERNING WITH AN EXCIMER LASER

MATERIALS PATTERNING WITH AN EXCIMER LASER

By

EDWARD E. GUZZO, B.Sc.

A Thesis

Submitted to the School of Graduate Studies

in Partial Fulfilment of the Requirements

for the Degree

Master of Engineering

M^cMaster University

March, 1992

MASTER OF ENGINEERING (1992)
(Engineering Physics)

M^cMASTER UNIVERSITY
Hamilton, Ontario

TITLE: Materials Patterning with an Excimer Laser

AUTHOR: Edward E. Guzzo, B.Sc. (University of Waterloo)

SUPERVISOR: Professor J.S. Preston

NUMBER OF PAGES: xiii,105

ABSTRACT

An investigation into the feasibility of laser ablation as a material selective removal technique was conducted. Polyimide films approximately 1 micron thick were prepared on silicon wafers. The ablation rate of these films as a function of laser fluence was studied. It was observed that a minimum threshold fluence of 67 ± 6 mJ/cm² had to be surpassed to achieve a significant material removal rate. In addition to polyimide, the removal and damage characteristics of aluminum films were also examined. These films, which ranged in thickness from 50 to 1000 nm, were deposited on polyimide coated silicon wafers. It was found that the best results were produced by a single shot removal technique, with the quality of the hole dependent upon the incident fluence. At lower fluences, removal ceased and only physical damage to the film occurred. In an attempt to characterize this damage, the electrical resistance of small aluminum wires was monitored as they were exposed to laser pulses. It was found that a change in the resistance of the wires could not be detected prior to the onset of visible damage.

Once the optimal removal fluences for both materials were determined, a multilayer consisting of an aluminum layer "sandwiched" between two polyimide layers was prepared. By varying only the incident fluence, it was possible to remove upper layers without removing or damaging the underlying ones. In a related experiment, the possible incubation of polyimide by low fluence laser pulses was also examined.

ACKNOWLEDGEMENTS

I would like to thank my supervisor, Dr. John Preston, for his invaluable guidance and many helpful suggestions. I would also like to thank all of the graduate students in my lab for their day to day assistance over the past two years. I would especially like to thank my parents, Helen and Elio, whose support and encouragement over the years has been unending.

TABLE OF CONTENTS

	Page
1. Introduction	1
2. Theory	
2.1 Absorption of Light in Solids	6
2.1.1 Metals	6
2.1.2 Non-metals	8
2.2 Polymer Ablation	9
2.3 Incubation in Polymers	13
2.4 Removal of Metal Films	14
3. Experimental Procedure	
3.1 An Overview	16
3.2 Laser Ablation Apparatus	16
3.3 Sample Preparation	
3.3.1 Polyimide on Silicon	20
3.3.2 Aluminum on Polyimide on Silicon	20
3.3.3 The Polyimide and Aluminum Multilayer	21
3.3.4 Aluminum Wires	21
3.3.5 Free Standing Polyimide	22

	Page
3.4 Experimental Technique and Characterization	
3.4.1 Polyimide Ablation	24
3.4.2 Removal and Damage of Aluminum Films	24
3.4.3 Selective Ablation of the Multilayer	26
3.4.4 Resistance Measurements	27
3.4.5 Incubation of Polyimide	29
4. Results and Discussion	
4.1 Polyimide Ablation	33
4.2 Removal and Damage of Aluminum Films	44
4.3 Selective Ablation of the Multilayer	64
4.4 Incubation of Polyimide	74
4.5 Resistance Measurements as a Damage Indicator	80
5. Conclusions	87
6. Appendices	
A. Graphs of the ablated depth versus the number of incident pulses for polyimide at various laser fluences.	91
B. Calculation of the temperature rise in the section of an aluminum layer exposed to a single incident pulse.	100
7. References	102

LIST OF FIGURES

	Page
Figure 2.1	The chemical structure of polyimide. 10
Figure 3.1	Schematic of the experimental apparatus. 18
Figure 3.2	Diagram of the polyimide and aluminum multilayer. 23
Figure 3.3	Diagram of the mask needed for photolithography. 23
Figure 3.4	Preparation of a free standing polyimide film. 25
Figure 3.5	Diagram showing selective removal of metallic and dielectric layers. 28
Figure 3.6	Resistance measurements of the patterned aluminum wires. 30
Figure 3.7	Holder for the free standing polyimide film used in the incubation experiment. 31
Figure 4.1	Ablated depth versus number of laser pulses for polyimide at an incident fluence of 187 mJ/cm^2 . 34
Figure 4.2	Ablated depth versus number of laser pulses for polyimide at an incident fluence of 118 mJ/cm^2 . 36
Figure 4.3a	Surface profile of a hole produced by two successive pulses at a fluence of 187 mJ/cm^2 . 37
Figure 4.3b	Surface profile of a hole produced by eight successive pulses at a fluence of 187 mJ/cm^2 . 37

	Page
Figure 4.4a	SEM image of the polyimide surface prior to irradiation. 39
Figure 4.4b	SEM image of the bottom of a hole produced by four pulses at a fluence of 187 mJ/cm ² . 39
Figure 4.4c	SEM image of the underlying silicon surface following ablation of the polyimide layer. 40
Figure 4.5	The ablation rate of polyimide as a function of the incident fluence. 41
Figure 4.6	Cracking and S.S.R. threshold fluences for various thicknesses of aluminum. 45
Figure 4.7a	Photograph of a hole produced in a 235 nm thick aluminum layer by a single pulse at a fluence of 650 mJ/cm ² . 48
Figure 4.7b	SEM image of the edge of the hole shown in Figure 4.7a. 48
Figure 4.7c	SEM image of the damaged region of the hole shown in Figure 4.7a. 49
Figure 4.7d	SEM image of debris at the bottom of the hole shown in Figure 4.7a. 49
Figure 4.8	EDXS scan showing the composition of the debris at the bottom of the hole in Figure 4.7a. 50
Figure 4.9a	Photograph of a hole produced in a 235 nm thick aluminum layer by a single pulse at a fluence of 326 mJ/cm ² . 52

	Page
Figure 4.9b SEM image of the bottom of the hole shown in Figure 4.9a.	52
Figure 4.9c SEM image showing the edge quality of the hole in Figure 4.9a.	53
Figure 4.10a Photograph of a hole produced in a 235 nm thick aluminum layer by a single pulse at a fluence just above the S.S.R. threshold.	54
Figure 4.10b SEM image showing the edge quality of the hole in Figure 4.10a.	54
Figure 4.11a Photograph of a hole produced in a 235 nm thick aluminum layer by a single pulse at a fluence just below the S.S.R. threshold.	56
Figure 4.11b SEM image showing cracking and partial removal of the aluminum in the damaged region in Figure 4.11a.	56
Figure 4.11c SEM image showing a region (in Figure 4.11a) where the aluminum has been peeled back by the incident pulse.	57
Figure 4.11d Magnification of Figure 4.11c, showing debris on the surface of the underlying polyimide.	57
Figure 4.12 EDXS scan of the composition of the debris remaining on the underlying polyimide surface in the region shown in Figure 4.11d.	58

	Page
Figure 4.13 The onset of cracking as a function of incident fluence for various thicknesses of aluminum.	60
Figure 4.14a Photograph of damage to a 470 nm thick aluminum layer caused by two incident pulses at a fluence of 265 mJ/cm ² .	62
Figure 4.14b Photograph of damage to a 470 nm thick aluminum layer caused by ten incident pulses at a fluence of 265 mJ/cm ² .	62
Figure 4.15a Photograph of a hole ablated through the upper layer of a multilayer.	66
Figure 4.15b Surface profile of the hole shown in Figure 4.15a.	66
Figure 4.15c SEM image showing the bottom surface of the hole in Figure 4.15a.	67
Figure 4.15d SEM image showing the surface of a section of the aluminum layer which has not been irradiated.	67
Figure 4.15e SEM image of debris surrounding the hole shown in Figure 4.15a.	68
Figure 4.16a Photograph of a hole which penetrates through both the upper polyimide and aluminum layers.	70
Figure 4.16b Surface profile of the hole shown in Figure 4.16a.	70
Figure 4.16c SEM image of the bottom of the hole shown in Figure 4.16a.	71

	Page
Figure 4.16d SEM image showing the edge quality of the hole in Figure 4.16a.	71
Figure 4.17a Surface profile of the silicon substrate following removal of the multilayer.	72
Figure 4.17b SEM image of the silicon surface shown in Figure 4.17a.	72
Figure 4.18 EDXS scan showing the composition of the debris remaining on the silicon surface after the multilayer has been removed.	73
Figure 4.19a Transmission through the free standing polyimide film as a function of wavelength prior to irradiation.	76
Figure 4.19b Transmission through the free standing polyimide film as a function of wavelength following irradiation.	77
Figure 4.20a Infrared transmission of the free standing film as a function of wavelength prior to irradiation.	78
Figure 4.20b Infrared transmission of the free standing film as a function of wavelength following irradiation.	79
Figure 4.21 Photograph of the free standing film following irradiation.	81
Figure 4.22a SEM image of a 10 micron wide wire irradiated with 40 laser pulses at a fluence of 96 mJ/cm ² .	83

	Page
Figure 4.22b Magnification of Figure 4.22a showing damage to a section of the aluminum wire.	83
Figure 4.22c Magnification of Figure 4.22a showing the region where the aluminum wire has been inadvertently lifted up, thereby revealing the underlying polyimide.	84
Figure 4.23 SEM image of a 100 micron wide wire exposed to a single laser pulse at a fluence of 121 mJ/cm ² .	86

LIST OF TABLES

		Page
Table 4.1	Experimental values for the ablation threshold and the absorption coefficient of polyimide.	42
Table 4.2	Removal and cracking thresholds for various thicknesses of aluminum.	47
Table 4.3	The number of incident pulses (at a given fluence) required to cause damage in aluminum layers of various thicknesses.	61

1. INTRODUCTION

Lasers offer a unique and flexible source of light for many applications. Output powers from milliwatts to greater than megawatts are available. This power can be delivered as either a continuous wave or as a series of pulses, with pulse lengths as short as 10^{-14} seconds. In addition, laser light is highly collimated and nearly monochromatic. As a result, the laser beam can be focused down to a small spot, the size of which is ultimately limited only by diffraction effects.

In the field of laser processing, the terms ablation and etching are often used interchangeably. However, there are several differences between the two processes. Etching is a material removal process in which the laser light either photochemically or thermally enhances a chemical etching process. The etching is performed in the presence of an external liquid or gaseous etchant which is selected to undergo a particular chemical reaction with the material. The laser light elevates the etch rate in the irradiated area and there is typically no threshold which must be surpassed for the reaction to proceed. As a result, low laser intensities are generally sufficient for etching. Ablation on the other hand, refers to material removal due solely to the interaction of the laser light with the material. It is essentially a physical removal process rather than a chemical one, although the material may undergo some chemical modification during ablation. Ablation is performed in air or in vacuum and without the use of external etchants. In addition, an intensity threshold must be surpassed in order to achieve

ablation. Below this threshold, the ablation rate is negligible. As a consequence of the threshold, ablation generally requires higher laser intensities than does etching.

Laser processing with excimer lasers offers many advantages for materials patterning. Thermal damage to the sample is minimized, enabling even temperature sensitive materials to be patterned. The ablated material carries away thermal energy rather than allowing it to be transferred to the bulk. Confirmation of this fact is provided by thermocouple experiments which reveal that sample heating tapers off to a constant value above the ablation threshold¹. Since the output wavelength of an excimer laser is in the ultraviolet range, it is possible to achieve sub-micron resolution in the patterning of materials. In addition, quick patterning of large areas is possible since the sample need not be placed in any solutions or in a vacuum system. By inserting a predesigned mask into the laser beam, many patterns may be produced simultaneously.²

Ablation is found to work quite well as a processing technique for a particular class of compounds known as polymers³. Ablation studies under different conditions and using different laser wavelengths have been performed on many polymers including common ones such as polyethylene terephthalate (PET)⁴, polymethylmethacrylate (PMMA)⁵, polyimide^{6,7} and photoresist⁸. Both polyimide and photoresist have important technological applications. Polyimide is used as a passivation layer and to a greater extent as a dielectric in the separation of metallic multilayers and interconnects. Photoresist is used almost exclusively as a masking layer during the processing steps involved in microelectronic fabrication. Ablation has also been performed on the two

most common semiconductors, GaAs⁹ and Silicon¹⁰, but the results are not as promising as they are for polymers.

The advantages possessed by excimer lasers have opened up a wide range of applications for laser ablation. One of the most recent applications is the drilling of via holes to interconnect metal layers in a metal-dielectric-metal multilayer¹¹. Since the dielectric used in these multilayers is often polyimide, laser ablation is a technique well suited to this process. The technique has worked so well that it is currently being used on a production line¹². The excimer laser is also useful in the cleaning of surfaces. In particular, the ablation of resists from alignment mark areas has been performed in order to improve alignment from one processing step to the next^{13,14}.

The removal of metal films¹⁵ and in particular those which make up electrical circuits¹⁶ has also been investigated. In this process, the laser is used to modify an existing circuit by severing the connection between devices. Thus, a generalized circuit can be tailored after fabrication to suit a specific application.

Perhaps one of the most valuable future uses of ablation will be in excimer laser lithography¹⁷. Traditional lithography and etching involves two steps. Photolithography is initially performed which transfers an image of the mask onto the sample. Next, a suitable etching technique is selected to remove any exposed material which is not covered by the photoresist. In excimer laser lithography, the conventional light source is replaced by an excimer laser. Excimer lasers are much more powerful and operate at shorter wavelengths than conventional sources, resulting in superior resolution. In

addition, excimer lasers offer the possibility of dry (resistless) patterning. The laser pulse passes through either a projection or a contact mask, ablating parts of the sample which are exposed while leaving masked areas undamaged. Since this single step process combines lithography and etching, it is quicker than traditional methods.

Materials processing and patterning using excimer lasers requires a detailed knowledge of both the ablation and damage characteristics of materials. Although ablation is easy to measure, a quantitative analysis of damage can be difficult to define and assess. Discolourations of exposed material may not be considered damage while visible cracking of the sample might. If, however, these cracks form over a successive number of laser pulses, then the exact number of pulses elapsed before one can say that damage has occurred is subjective.

Previous work has been performed by Singleton *et al*¹⁸ to determine the ablation and damage thresholds of several materials currently used in the fabrication of microelectronics. Their experiments were performed on thin films of various materials deposited on silicon wafers. They concluded that it was impossible to ablate polyimide while simultaneously exposing an aluminum layer to the same laser beam without causing damage to the aluminum. This is due to the low damage threshold of aluminum. However, in the ablation of via holes in polyimide with copper interlayers¹², it was observed that the ablation terminated upon reaching the copper surface. Although a polyimide and copper multilayer differs from a polyimide and aluminum one, it does suggest that in some circumstances, a material selective removal process may be possible.

The main objective of this research is to explore the possibility of a material selective removal process for the production of holes in a polyimide and aluminum multilayer. It was hoped that a method could be developed to either selectively stop at a particular layer or remove it by simply varying the incident laser fluence. In addition, damage to underlying and nearby material must be held to a minimum. Initial experiments were performed on thin films of polyimide and aluminum in order to determine the removal and damage characteristics of these materials. Once these parameters were determined, a polyimide and aluminum multilayer was fabricated and selective removal was attempted. In a related experiment, the possible incubation of polyimide by low fluence laser pulses was also examined.

2. THEORY

2.1 ABSORPTION OF LIGHT IN SOLIDS

The absorption of light in a solid can be described by Beer's Law, which relates the intensity at a particular depth (x) into the solid to the incident intensity at the surface.

This law is expressed as:

$$I(x) = I_0 e^{-\alpha x} \quad (2.1)$$

where I_0 is the incident light intensity, $I(x)$ is the light intensity at a specific depth x into the solid and α is the absorption coefficient, which is a material property indicating the strength of optical attenuation.

2.1.1 METALS

Metals can be distinguished from insulators by their loosely bound outer shell electrons. These electrons are delocalized and are free to move about throughout the metal. When longer wavelength light (typically 1 micron or longer) is incident upon a metal, the optical properties are dominated by these free electrons. This results in strong attenuation of the incident light and is characterized by a high reflectivity. Insight into the optical characteristics of a particular material is provided by the material's penetration depth or skin depth. This is defined as the distance into the material at which the light intensity has dropped to e^{-1} (36.8%) of its incident value. This depth is given by¹⁹:

$$d_s = \frac{\lambda}{4\pi k} \quad (2.2)$$

where λ is the wavelength of the incident light and k is the extinction coefficient, a measure of the strength of optical attenuation within the material. At a wavelength of 1.03 microns, the skin depth in aluminum is approximately 8.2 nm.

As the wavelength of the incident light is decreased (into the visible and ultraviolet part of the spectrum), the free electron contribution to the optical properties diminishes and interband absorption begins to dominate. In general, the reflectivity of metals is reduced in the ultraviolet, but is dependent on the details of the band structure. In aluminum, at an incident wavelength of 310 nm, the reflectivity is 92.5%²⁰ and the skin depth is approximately 6.6 nm. Therefore, in films as thin as 50 nm, less than 0.01% of incident light will be transmitted.

Once the incident photon has been absorbed, its energy is quickly distributed (on the order of picoseconds) to the lattice via collisions and scattering. As a result, this energy provides rapid local heating of the metal. On the timescale of the incident pulse, the heat produced within the skin depth will diffuse a distance d_{th} , which is given by:

$$d_{th} = 2\sqrt{D_{th}t} \quad (2.3)$$

where D_{th} is the thermal diffusion constant and t is the duration of the incident laser pulse. For a 20 ns pulse absorbed in aluminum ($D_{th} = 1.01 \text{ cm}^2/\text{s}$), this diffusion length

will be about 2.8 microns. This distance is more than 400 times the optical skin depth at 308 nm. In addition, the thermalization time is about three orders of magnitude shorter than the pulse duration. As a result, it is reasonable to conclude that in films a micron thick or less, the laser pulse uniformly heats the film within the irradiated area.

2.1.2 NON METALS

Non-metals, including insulators and semiconductors, have optical properties different from metals mainly because they do not have a substantial number of free carriers. In contrast to metals, their outermost electrons are tightly bound to the nucleus. These materials have a band gap, which refers to the energy difference between the top of the valence band and the bottom of the conduction band. If photons with an energy greater than this gap are incident upon the material, they will be able to promote electrons across the gap and into the conduction band, thus creating a significant number of free carriers. This results in strong optical absorption. In the case of incident photons with energies less than the band gap, the photons are not absorbed by the material because they cannot promote electrons across the gap and the material appears transparent. The low light intensity absorption coefficient of polyimide at a wavelength of 308 nm is $1 \times 10^5 \text{cm}^{-1}$.⁶ This results in a skin depth of approximately 100 nm, which is about 15 times greater than in aluminum at the same wavelength.

2.2 POLYMER ABLATION

Polymers are a unique group of organic materials in that the molecules themselves are extremely large, consisting of 10^3 to 10^5 atoms. They are mainly composed of carbon, oxygen, nitrogen and hydrogen arranged into small molecular groups known as monomers. Each monomer consists of 6 to 40 atoms, with as many as 1000 monomer units linked together to form the polymer molecule²¹. In Figure 2.1, a typical monomer unit for polyimide is shown.

The actual mechanism of laser ablation can be divided into 3 processes: absorption of photons, material dissociation and material ejection. A temporal distinction between these processes is difficult since all three will occur during a nanosecond laser pulse. Absorption of an incident ultraviolet photon within the polymer may promote a bonding electron into an excited state, whereas a visible or infrared photon will generally have insufficient energy to initiate such a transition. Once the photon has been absorbed, one of two things may occur. If the excitation is to an energy level above the bond dissociation energy, then the molecule may dissociate at the next molecular vibration (within several picoseconds). This is known as a photochemical process since the absorbed photon causes direct bond breaking within the material. Another possible process occurs if the energy of the photon is internally converted into a vibrational excitation and is dissipated into surrounding molecules. If this thermal energy is then absorbed by one of the weakest bonds in the molecule, it may cause the molecule to thermally decompose. This process is associated with a temperature increase in the film

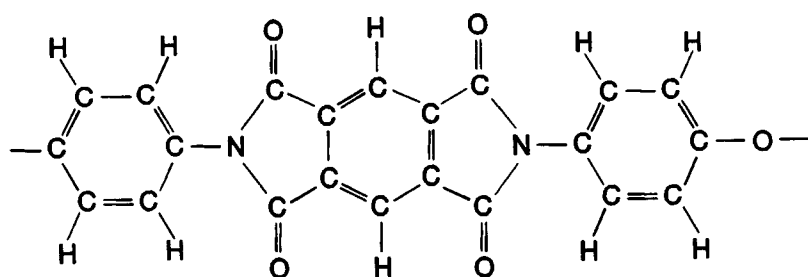


Figure 2.1 The chemical structure of a single monomer of polyimide. This structure is repeated up to 1000 times to form the polyimide molecule. It is also possible that the oxygen atom bonded to the benzene ring (on the right side of the diagram) may be replaced by a CH_2 group in some cases.

and is referred to as a photothermal process, since the photons act as a source of thermal energy.

Once the molecule has dissociated, either photochemically or photothermally, there will be a massive pressure increase within the material since the volume of dissociated fragments is greater than the molecule as a whole. This results in an explosive removal in which the ejected fragments can reach velocities of up to 10^5 m/s²². One of the unique characteristics of laser ablation is the existence of an ablation threshold. This refers to a lower fluence limit, expressed as energy per unit area per laser pulse (usually mJ/cm²), below which the rate of material removal is essentially zero.

The first set of experiments to determine the microscopic ablation mechanism was performed by Andrew *et al*³. They showed that in their fluence range, the ablation rate could be modelled by Beer's Law to yield:

$$d = \frac{1}{\alpha} \ln\left(\frac{E}{E_T}\right) \quad (2.4)$$

where E is the incident fluence, E_T is the threshold fluence, α is the absorption coefficient of the material and d is the ablated depth per pulse at the incident fluence E. The authors claim that the ablation mechanism is a thermal process due to the existence of an ablation threshold. They argue that if direct bond breaking was occurring within the material, then the ablation mechanism should not be dependent upon an ablation

threshold, but rather upon the total dose of incident energy. Their experiment, in which they applied sub-threshold multiple pulses to their films, showed no dependence on total dose. In addition, the authors irradiated a sample which had a miniature thermocouple mounted on it. Their results showed that all of the absorbed energy appeared as an increase in temperature of the film. This has been verified by other researchers¹ for wavelengths of 193, 248 and 308 nm.

Brannon *et al*⁶ also suggest a photothermal model. Their data also fits well to Equation 2.4 over the range studied and their ablation threshold of 70 mJ/cm² at 308 nm compared well with Andrew's value of 60 mJ/cm². The authors also argue that since the bond dissociation energies for polyimide are estimated at between 5 and 8 eV, whereas a 308 nm photon has an energy of approximately 4 eV, it seems unlikely that photolysis due to single photon absorption is occurring. Since the energy for shorter wavelength photons is greater, it is possible that they may induce photolysis within the material. Their data also indicated that the absorbed energy per unit volume needed to initiate ablation was equal for the examined wavelengths of 193, 248 and 308 nm, again suggesting a photothermal mechanism.

Other groups of researchers including Srinivasan *et al*⁷ claim that the ablation mechanism is photochemical. Their data does not fit well to Equation 2.4 over the fluence range examined in their experiment. In addition, they performed mass spectroscopy on the ablated products and discovered that HCN was being produced. They calculated the temperature rise within the film and showed that at these

temperatures, the rate of HCN production was far greater than could be produced by thermolysis. The authors therefore suggest that the ablation process is a multiphoton photochemical one, based on the above evidence and on the fact that at laser fluences of 300 mJ/cm^2 , there could be up to 9 photons absorbed per monomer in the ablated volume.⁷

At present, there is still debate as to which is the correct ablation mechanism. The expression of Beer's Law for the ablated depth (Equation 2.4) appears to hold true only at low fluences. The dominant ablation process is dependent upon material properties and in many cases both photolysis and thermolysis will occur simultaneously. The wavelength (and therefore the energy) of the incident photons also plays a role in the mechanism. As a general rule, shorter laser wavelengths favour photoinduced mechanisms, while longer wavelengths favour thermal ones. This trend is reflected in a reduction of the ablation threshold at shorter wavelengths. Other effects such as pulse length, non-linear processes, saturation of the absorption, shielding of the film by the ablated plume, and possible incubation of the film must all be accounted for to quantitatively describe the ablation mechanism.

2.3 INCUBATION IN POLYMERS

The incubation of polymers prior to their ablation has been observed by several groups^{23,24}. Incubation involves fracturing chemical bonds within the polymer. The initial laser pulse incident upon the polymer is unique since virgin material is exposed.

During subsequent pulses, the material immediately beneath the ablated area has been exposed to lower laser fluences which have not caused ablation, but may have altered the material in some fashion. Incubation may change the optical as well as the chemical properties of the material. As a result, the absorption coefficient of the material could vary as incubation proceeds. It is also possible that the production of photofragments under the surface of the film will continue until a sufficient number has accumulated to cause material ejection. At present, evidence for the possible incubation of polyimide by 308 nm low fluence pulses has not been found.

2.4 REMOVAL OF METAL FILMS

The primary advantage of using an excimer laser for metal film processing is that the reflectivity of metals in the ultraviolet region of the spectrum is generally lower than in the visible or infrared, thus allowing greater coupling of the optical energy into the film. Some of the earliest experiments on processing metallic films with an excimer laser were performed by Andrew *et al*¹⁵. In their experiments they used a XeCl excimer laser to remove thin (120 nm) aluminum films from mylar and glass substrates. They employed a single shot removal technique in which a single laser pulse removed the entire thickness of aluminum in the irradiated region. This technique worked quite well as indicated by the lack of thermal damage to the substrate near the irradiated zone. In addition, x-ray fluorescence as well as optical and electron microscopy revealed that little residual aluminum debris remained at the metal-substrate interface subsequent to the

removal.

An interesting result of these experiments was that the removal threshold for the films was lower than their vaporization curves. This indicated that some process other than evaporation of the metal was occurring. This was confirmed by Lazare *et al*²⁵. Their results showed that the removal threshold varied linearly with the thickness of the aluminum layer, indicating a bulk rather than a surface process. It appears as though a bulk threshold temperature may have to be reached before material removal will occur.

Both groups of authors agree on the mechanism of the removal process. They believe that the incident photons are absorbed by the metal and converted into heat. Given the large thermal diffusion coefficient of the metal (see section 2.1.1), and the fact that the films themselves are quite thin, a temperature rise in the film occurs almost instantly. In addition, the dielectric substrate has a small thermal diffusion coefficient, essentially confining all of the energy within the metal layer. The heating of the metal may cause thermal decomposition of any impurities near the metal-substrate interface, or of the substrate itself. This would result in a large pressure build-up at this interface, followed by an explosive type ejection of the entire metallic layer.

3. EXPERIMENTAL PROCEDURE

3.1 AN OVERVIEW

Initial experiments were performed to determine the ablation rate of polyimide as a function of laser fluence. Following this, the removal and damage characteristics of aluminum thin films as a function of both thickness and laser fluence were examined. To further characterize damage, the resistance of narrow aluminum wires was monitored as they were exposed to incident laser pulses. This was done in an attempt to observe a resistance change prior to the onset of visible damage. Once the processing characteristics of both polyimide and aluminum were determined, a multilayer consisting of alternating layers of these materials was prepared. The possibility of removing certain layers without removing or damaging underlying layers was examined. Scanning electron microscopy (SEM) was performed to examine the surface quality of the samples following this processing.

The possible incubation of polyimide by 308 nm laser light was also studied. A free standing polyimide film was prepared and exposed to multiple low fluence laser pulses. Infrared and ultraviolet spectroscopy was performed prior to and following irradiation to see if chemical or optical changes in the film had occurred.

3.2 LASER ABLATION APPARATUS

The laser used in this experiment was a Lumonics model TE-860-4 excimer laser.

The word excimer is a contraction of Excited Dimer, giving some indication of how this type of gas laser operates. A rare gas atom (eg. Ar, Kr, Xe) is combined in an excited state with a halogen atom (eg. F, Cl) to form a rare gas halide excimer. The transition to the ground state results in an output in the ultraviolet range of the spectrum.

Our particular laser was a XeCl excimer producing 20 nanosecond pulses at a wavelength of 308 nm, with a beam cross section of 4 cm by 2 cm. The energy per pulse was approximately 200 mJ with a maximum fluctuation of $\pm 10\%$ from pulse to pulse. The pulse repetition rate of the laser was variable up to 200 Hz. A single shot mode was also available, which allowed remote manual triggering of the laser from the target area. Manual triggering was used for most trials, except for those which required hundreds of pulses to complete.

The experimental set-up is shown in Figure 3.1. The laser pulses were passed through a 0.5" diameter aperture so that 1" optics could be used. The pulses passed through a series of neutral density filters which allowed their power to be varied. After the filters, a second aperture approximately 1.2 mm in diameter was used to select the uniform central portion of the output. The laser pulse was then focused down using a 1" diameter plano-convex lens with a focal length of 2.5 cm. The lens was mounted on a translation stage so that the sample to lens distance could be altered. By adjusting this distance, the image of the aperture could be properly focused on the sample. A stereoscopic microscope (Seiwa model SKZ-4) was incorporated into the system, permitting *in situ* observation of the ablation.

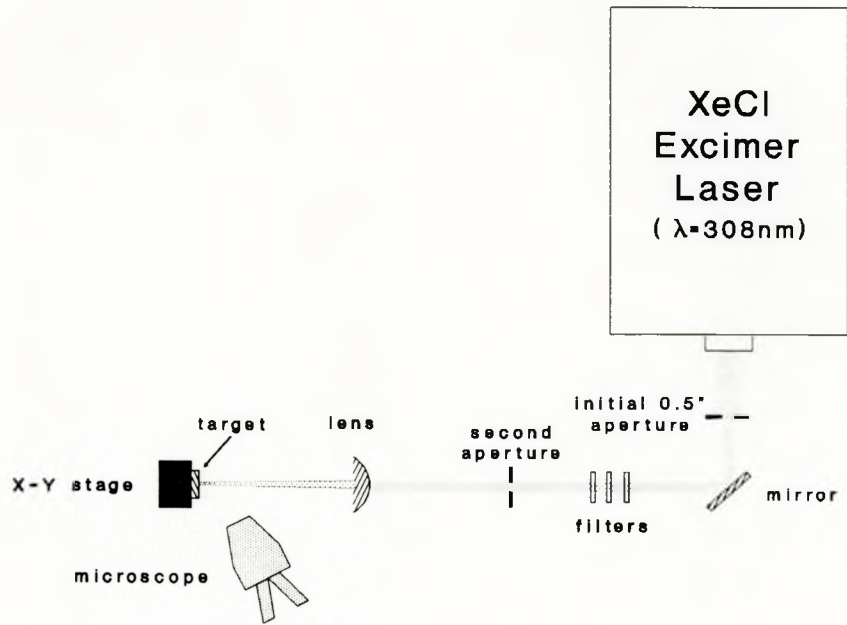


Figure 3.1 Schematic of the experimental apparatus.

The samples were mounted onto a metal plate with vacuum grease allowing them to be quickly and easily changed. The metal plate was fastened to an x-y translation stage which permitted any part of the sample to be positioned in the beam path. When used in conjunction with the microscope, the translation stage allowed very precise positioning of the sample and therefore of the ablated holes. Focusing of the image was accomplished by ablating several test holes in the polyimide sample, each at a slightly different focus. The image was focused correctly when the ablated hole was circular with sharply defined edges. A demagnification ratio of 4:1 was selected, based on a compromise between the maximum possible power delivered to the sample and the edge quality of the ablated hole. It was observed experimentally that a larger demagnification ratio produced holes with poorly defined edges while a smaller demagnification ratio limited the maximum attainable fluence to a lower value. The size of the second aperture was determined by the spatial uniformity of the laser beam and more importantly by the desired spot size on the sample. Our particular combination of aperture size and demagnification ratio resulted in a final image size of about 250 microns at the surface of the sample.

The pulse energy was measured before each trial. This was accomplished by inserting a mirror into the beam path between the second aperture and the focusing lens and redirecting the beam into a power meter (Scientech model 365). The depth, diameter and surface profile of the ablated holes was measured using a mechanical surface profilometer (Tencor Alpha-step model 200). Given the pulse energy transmitted through

the second aperture and the diameter of the ablated hole, the fluence at the sample surface could be calculated. Typically, the maximum possible fluence was approximately 650 mJ/cm².

3.3 SAMPLE PREPARATION

3.3.1 POLYIMIDE ON SILICON

The first set of experiments was performed on thin films of polyimide in order to determine its ablation rate as a function of fluence. The films were prepared by spin coating a liquid polyimide formulation (CIBY-GEIGY Probimide™ 200 series polyimide) onto clean 1.25" diameter <111> oriented silicon wafers. The polyimide is designed to yield uniform 1 micron thick films when applied at a spin speed of 4000 r.p.m. Subsequent to spinning, the films were cured on a hot plate for 30 minutes at 85°C, followed by 15 minutes at 150°C and finally for 15 minutes at 240°C. Most of the polyimide films described in this thesis were prepared in this manner, with the exception of the free standing polyimide films which were prepared using a slightly different technique (see section 3.3.5).

3.3.2 ALUMINUM ON POLYIMIDE ON SILICON

In the second stage of experimentation, the removal and damage characteristics of aluminum films were examined. The substrates were polyimide coated silicon wafers

as described in section 3.3.1. The aluminum (99.999% pure) was thermally evaporated onto the wafers at a pressure of 10^{-5} Torr or lower, giving films ranging in thickness from 50 nm to 1000 nm. A precise measurement of the aluminum layer thickness was obtained after deposition using the surface profilometer.

3.3.3 THE POLYIMIDE AND ALUMINUM MULTILAYER

The polyimide-aluminum-polyimide multilayer was produced on a silicon wafer by the successive deposition of 1 micron of polyimide, 470 nm of aluminum and another 1 micron polyimide layer, employing the techniques described in the previous two sections. A diagram of this multilayer is shown in Figure 3.2.

3.3.4 ALUMINUM WIRES

In the next phase of experimentation, the effect of damage on thin aluminum wires was studied. These wires were prepared in the following manner. A 450 nm thick aluminum layer was deposited on a polyimide coated silicon wafer. A layer of positive photoresist (Shipley Microposit S-1400) was spun on top and soft baked for 30 minutes at 100°C.

A mask was designed which consisted of 26 independent patterns. Each pattern was a 300 micron long wire terminated on each end by a 2 mm x 2 mm contact pad. The width of the wires varied from 500 microns to as little as 10 microns and their thickness was determined by the thickness of the deposited aluminum. A diagram of this

mask can be seen in Figure 3.3. A mask aligner (Karl Suss model MJB3) was used to expose the photoresist-covered sample through the mask. After exposure, the wafer was placed in a developer which removed the exposed photoresist. The next processing step would usually involve hard baking the sample and removing the exposed aluminum using an appropriate etching technique. Fortunately, the photoresist developer was also an effective aluminum etchant, so the hard bake and etching steps could be eliminated. The developer removed the entire aluminum film except beneath the photoresist, thereby transferring the mask pattern to the sample. The final step involved placing the wafer in a bath of photoresist stripper to remove the photoresist from the top of the patterned aluminum.

3.3.5 FREE STANDING POLYIMIDE

The free standing polyimide film needed for the incubation experiment was produced in the following manner. A 200 nm layer of spin-on-glass (Emulsitone Silicafilm SiO₂) was spin coated onto a clean glass slide and cured for 15 minutes at 200°C. A 1 micron polyimide layer was deposited on top of this layer using the technique described in section 3.3.1. The slide was placed in a dilute hydrofluoric acid and deionized water solution. This solution etched away the layer of spin-on-glass, but did not attack the polyimide. The polyimide layer remained intact and floated to the surface of the solution. A metal ring 18 mm in diameter was placed beneath the floating film and slowly raised until it supported the film. The film was rinsed with deionized

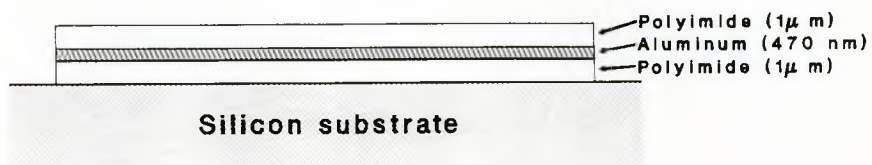


Figure 3.2 Diagram of a polyimide and aluminum multilayer deposited on a silicon substrate.

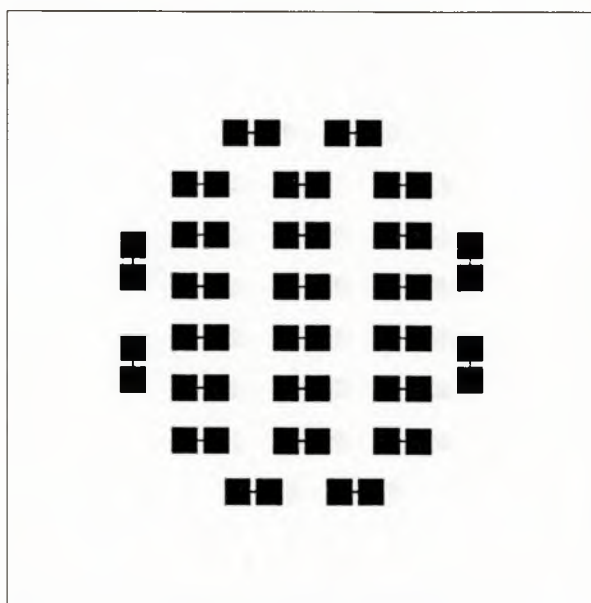


Figure 3.3 Diagram of the mask used during photolithography to pattern the aluminum wires needed for the resistance experiments.

water and dried in an oven. A schematic of this processing technique can be seen in Figure 3.4.

3.4 EXPERIMENTAL TECHNIQUE AND CHARACTERIZATION

3.4.1 POLYIMIDE ABLATION

The polyimide-on-silicon samples were mounted on the x-y translation stage as described in section 3.2. The sample was positioned in the beam path and a single laser pulse was applied. A new section of the sample was then moved into the beam path and two laser pulses (of the same fluence as the first) were applied. This process of applying an increasing number of shots per hole was continued until the final hole penetrated through the polyimide layer. This was determined visually with the stereomicroscope. The depth of the holes was measured with the surface profilometer and plotted to give the ablated depth as a function of the number of laser pulses. The slope of this curve provides the ablation rate per pulse for a given fluence. These experiments were then repeated for several different laser fluences in order to determine the ablation rate as a function of fluence.

3.4.2 REMOVAL AND DAMAGE OF ALUMINUM FILMS

Experiments were performed to determine the single shot removal (S.S.R.) threshold and the cracking threshold for aluminum films of various thicknesses.

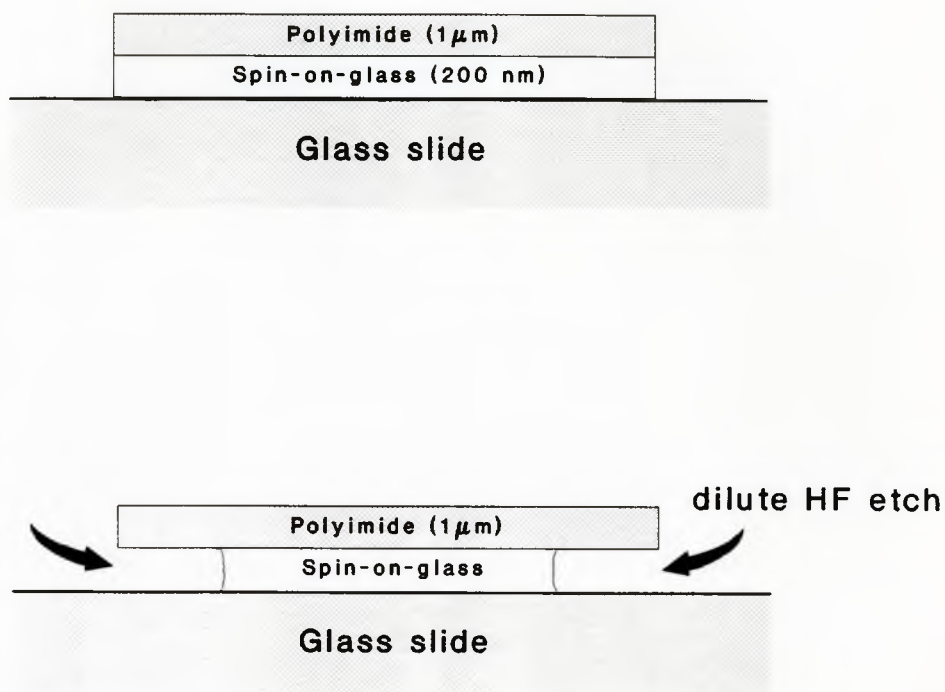


Figure 3.4 Preparation of a free standing polyimide film. The hydrofluoric acid etched the spin-on-glass, but did not attack the polyimide.

Determination of the S.S.R. threshold was straightforward. Different sections of the same film were exposed to a single laser pulse. The fluence of successive pulses was lowered until complete S.S.R. was no longer observed. This determination was easily made with the stereomicroscope.

The cracking threshold of these films was investigated by exposing them to laser fluences below the S.S.R. threshold. The cracking process was studied for single and multiple pulses (up to 1000) at various laser fluences and film thicknesses. In addition, SEM was performed on the films in order to reveal damage on a smaller scale. The cracking threshold was defined as the maximum fluence incident upon the aluminum surface for 1000 pulses without causing the formation of visible cracks which could be observed with an optical microscope.

3.4.3 SELECTIVE ABLATION OF THE MULTILAYER

The possibility of selectively removing different layers of the multilayer was investigated. It was hoped that by varying the incident fluence alone, certain layers could be removed without removing or damaging the underlying ones. Prior to this experiment, it was necessary to know suitable fluences for polyimide and aluminum removal as well as the damage threshold of aluminum. This information was obtained by the experiments outlined in sections 3.4.1 and 3.4.2. Initially, a fluence was chosen which was sufficient to ablate the top polyimide layer, but below the damage threshold of the aluminum layer. The approximate number of shots required to completely remove

the polyimide layer could be estimated from the ablation rate versus fluence curve. If the exposed aluminum layer was to be removed as well, a single pulse was then applied whose fluence was above the S.S.R. threshold for that particular thickness of aluminum. This pulse should completely remove the aluminum in the irradiated region but leave the underlying polyimide unaffected. If complete removal of the entire multilayer was desired, a sufficiently large fluence was chosen and the ablation performed. Since the ablation threshold for silicon is much higher than for polyimide or aluminum¹⁸, the ablation process should terminate at the silicon substrate. A diagram of this processing scheme can be seen in Figure 3.5.

3.4.4 RESISTANCE MEASUREMENTS

Resistance measurements were performed on the patterned aluminum wires as a method of electrically characterizing damage to the aluminum. Since the wires were thin and narrow (see section 3.3.4), any cracks which partially or completely severed the wire could be detected as an increase in the resistance of the wire. It was hoped that a change in the resistance could be correlated with a particular amount of induced damage. This method was chosen as a way of quantitatively measuring damage since visual observation is subjective. Given that the resistance of the narrowest wires was approximately 2Ω , a four point resistance technique was implemented to improve accuracy. Four moveable probes were mounted beside the translation stage. The probe tips could be manipulated into position and pressed into electrical contact with the aluminum pads using

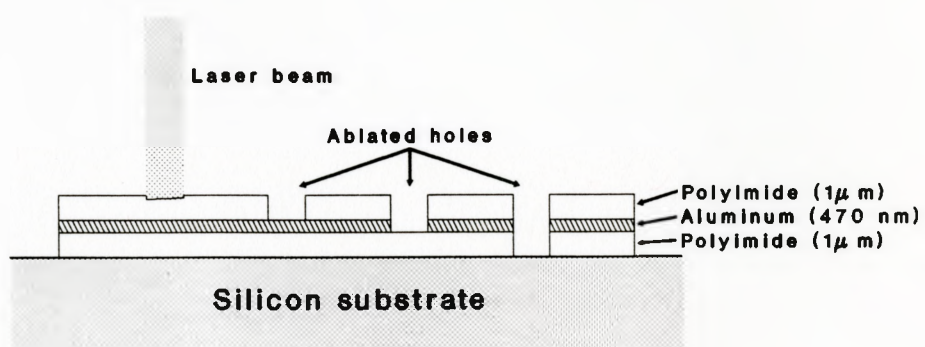


Figure 3.5 Diagram showing selective removal of the metallic and dielectric layers.

thumbscrews. The probes were connected to a digital multimeter (Keithley model 199) which measured the resistance. A laser fluence was selected based on the results of the experiments conducted in section 3.4.2. The wire was exposed to single and multiple pulses, while the resistance was monitored. This allowed *in situ* measurement of the wire's resistance without removing the sample or turning off the laser. The procedure was repeated for different fluences and numbers of pulses. A schematic of this set-up is shown in Figure 3.6.

3.4.5 INCUBATION OF POLYIMIDE

The free standing polyimide film was analyzed for incubation using ultraviolet, visible and infrared spectroscopy. The film was mounted in a specially designed holder (see Figure 3.7) and its infrared transmission spectrum was analyzed in an IR spectrophotometer (Perkin-Elmer model 283) before exposure to ultraviolet light. Following this, the ultraviolet and visible transmission spectrum of the film was measured using a UV/VIS/NIR spectrophotometer (Perkin-Elmer Lambda 9). There was a possibility that performing an ultraviolet transmission spectrum might inadvertently incubate the film, so a second infrared transmission spectrum was performed. Comparison of the two infrared spectra revealed no differences, and so it was concluded that measuring the ultraviolet transmission spectrum had no measurable effect on the film.

The next step was to see if low levels of laser light caused incubation. The film

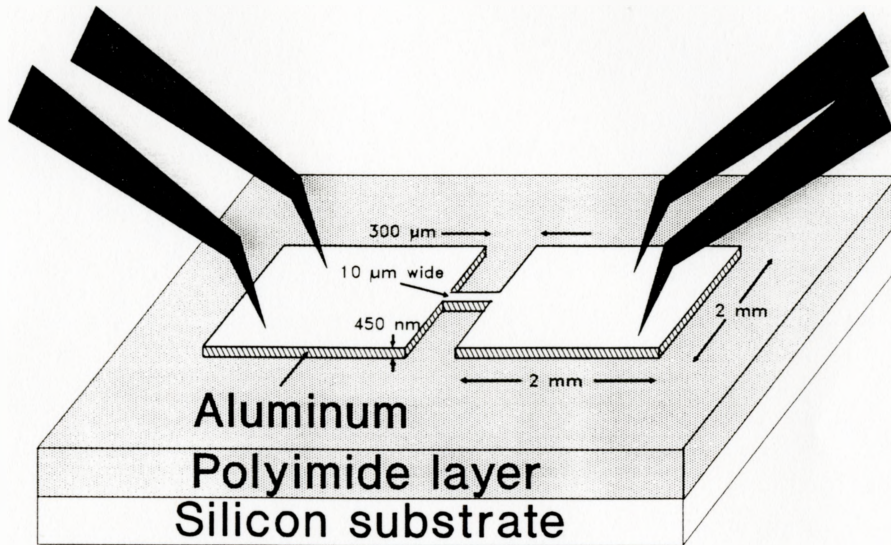


Figure 3.6 Diagram showing the probe tips in contact with a patterned aluminum wire. The wire was irradiated by the laser while its electrical resistance was monitored.

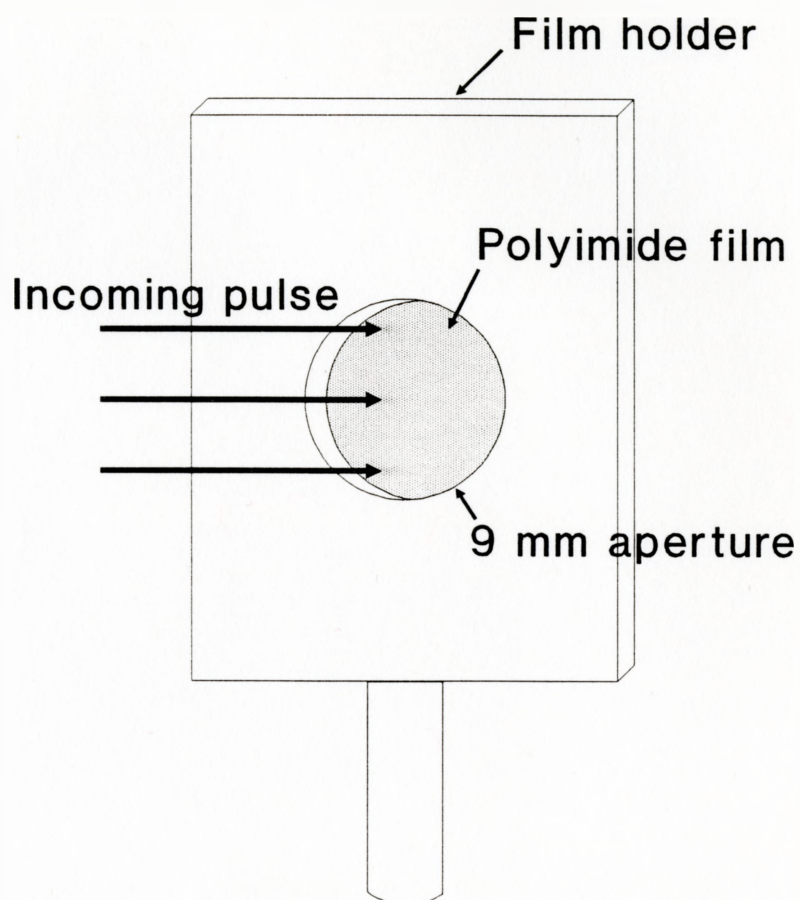


Figure 3.7 Holder for the free standing polyimide film used in the incubation experiment.

was exposed to sub-threshold pulses at a fluence of 28 mJ/cm^2 . Since the film was free standing, both sides could be irradiated by the laser. Given that the skin depth for polyimide is approximately 0.1 micron (see section 2.1.2) and the film was approximately 1 micron thick, irradiation of both sides would incubate a significant portion of the film. After exposure to a fixed number of pulses, both infrared and ultraviolet spectroscopy were again performed to see if any changes had taken place. This iterative procedure was repeated several times until each side of the film had received a total of 1000 laser pulses.

4. RESULTS AND DISCUSSION

4.1 POLYIMIDE ABLATION

The ablation rate of polyimide was measured in the manner described in section 3.3.1. Three separate trials were performed at each fluence to obtain the ablated depth as a function of the number of incident laser pulses. Figure 4.1 is a plot of the trials performed at a fluence of 187 mJ/cm^2 . At this fluence, the ablated depth approached the film thickness after six pulses, so only the first five laser pulses were used in the fit to obtain the slope. As expected, there was a linear relationship between the ablated depth and the number of pulses. The slope of the fit provides the ablation rate at that fluence. In Figure 4.1, the ablation rate is 0.150 ± 0.002 microns per pulse. The small x-intercept of the fit (0.006 ± 0.016 microns) passes within experimental error of the origin, which implies that at least in this case, incubation of the sample is not a prerequisite for ablation. However, it is possible that incubation is a subtle effect which cannot be detected in this type of experiment. It is also evident that the ablation terminates at a depth of 0.95 microns, which is the approximate thickness of the polyimide layer. This occurs because the incident fluence is insufficient to cause silicon ablation.¹⁸ Figure 4.2 is a graph of the ablated depth versus the number of laser pulses, performed at a fluence of 118 mJ/cm^2 . Again a linear relationship between the ablated depth and the number of pulses was observed. At this lower fluence it took approximately twice the number of pulses to penetrate through the polyimide, resulting

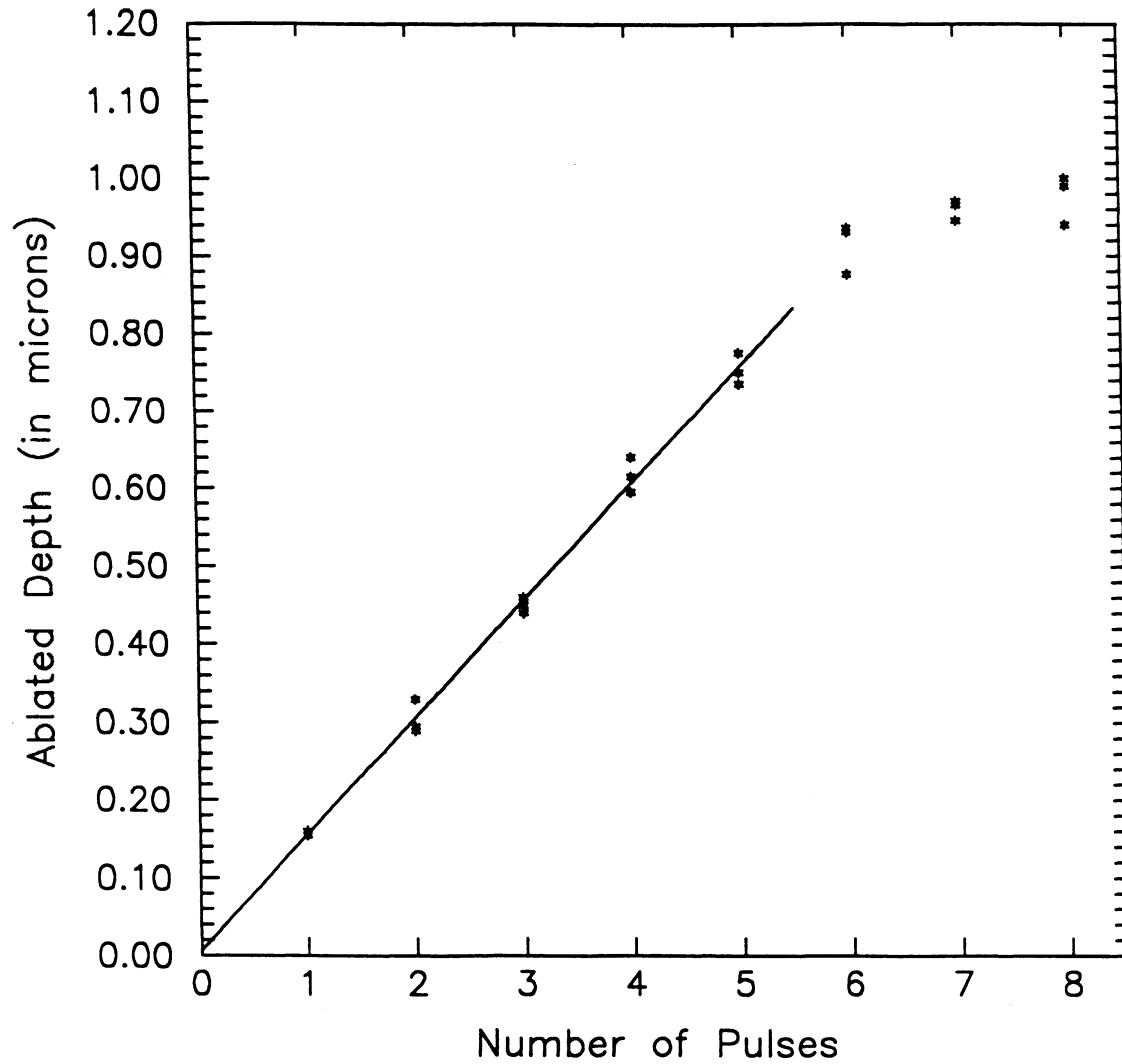


Figure 4.1 Ablated depth versus number of laser pulses for polyimide at an incident fluence of 187 mJ/cm^2 . The random errors present are reflected in the scatter of the data.

in an ablation rate of about 0.075 ± 0.002 microns per pulse. Similar plots for all the fluences examined can be seen in Appendix A.

In the experimental procedure, the central portion of the laser beam was selected so that the intensity profile across the beam diameter would be uniform. As a result, the depth of the ablated hole should also be uniform. Figure 4.3a is a surface profile of the bottom of a hole made by two successive pulses at a fluence of 187 mJ/cm^2 . It was noticed that across the entire 250 micron width of the hole, the depth varies by no more than $\pm 10\%$ from the average depth. This corresponded to a roughness of about ± 30 nm. Figure 4.3b is a profile of a hole made by 8 successive pulses at the same fluence as Figure 4.3a. This is actually a profile of the underlying silicon surface, since the hole penetrates through the polyimide. In both Figure 4.3a and 4.3b, there are small peaks on the surface of the polyimide near the edge of the ablated hole. These peaks vary in both size and shape and were present in most of the surface profiles. Their presence is the result of ablated debris which has redeposited on the polyimide surface surrounding the hole.

In order to observe the ablated holes on a microscopic scale, SEM was performed. Figure 4.4a is a SEM image of the polyimide surface prior to irradiation. The surface is smooth with the exception of a few dust particles. Figure 4.4b is a SEM image of the bottom surface of an ablated hole which partially penetrated the polyimide. This hole was created by 4 pulses at a fluence of 187 mJ/cm^2 . As expected, the surface quality at the bottom of the hole was worse than the surface of the unexposed polyimide.

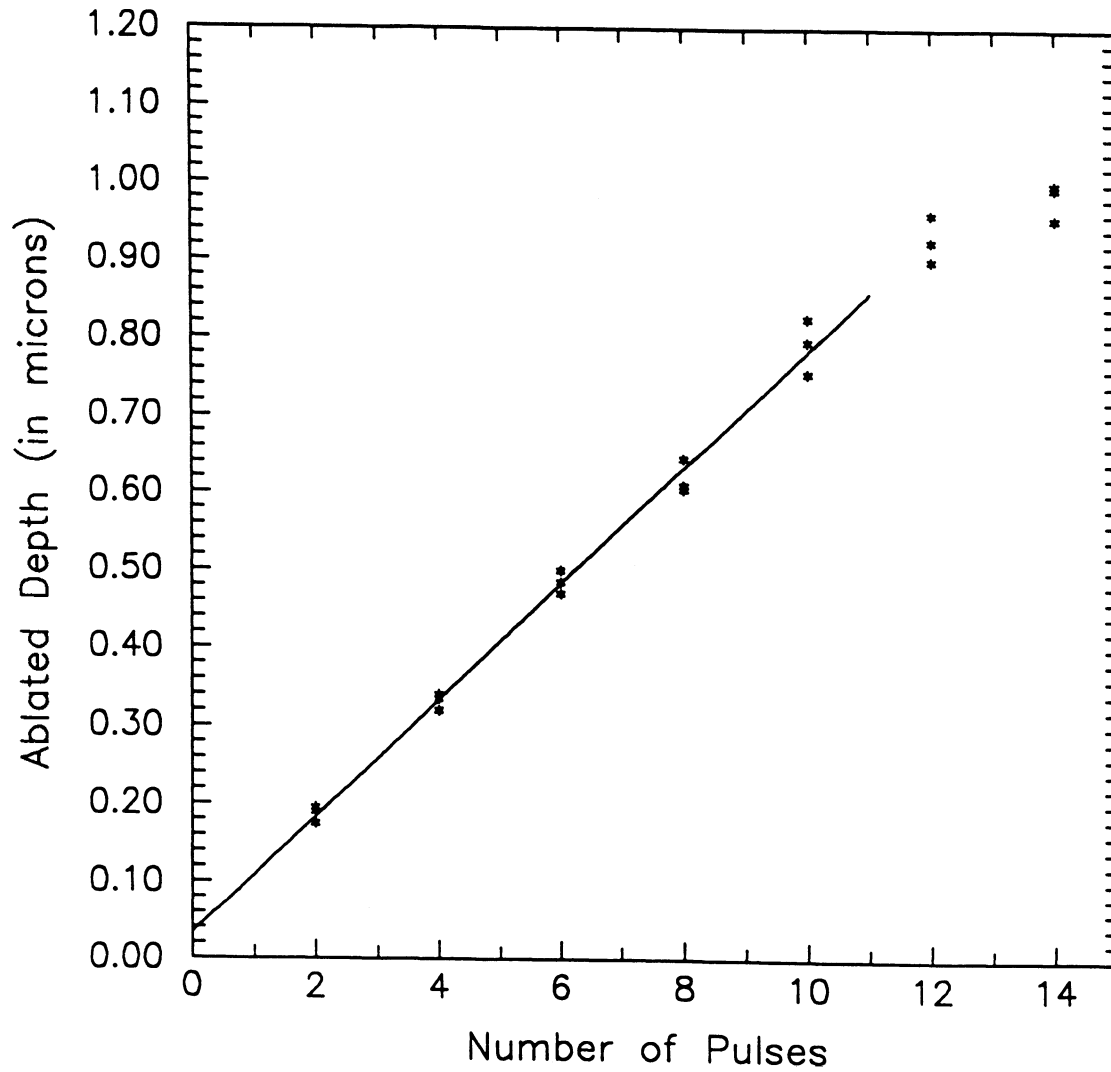


Figure 4.2 Ablated depth versus number of laser pulses for polyimide at an incident fluence of 118 mJ/cm^2 . The random errors present are reflected in the scatter of the data.

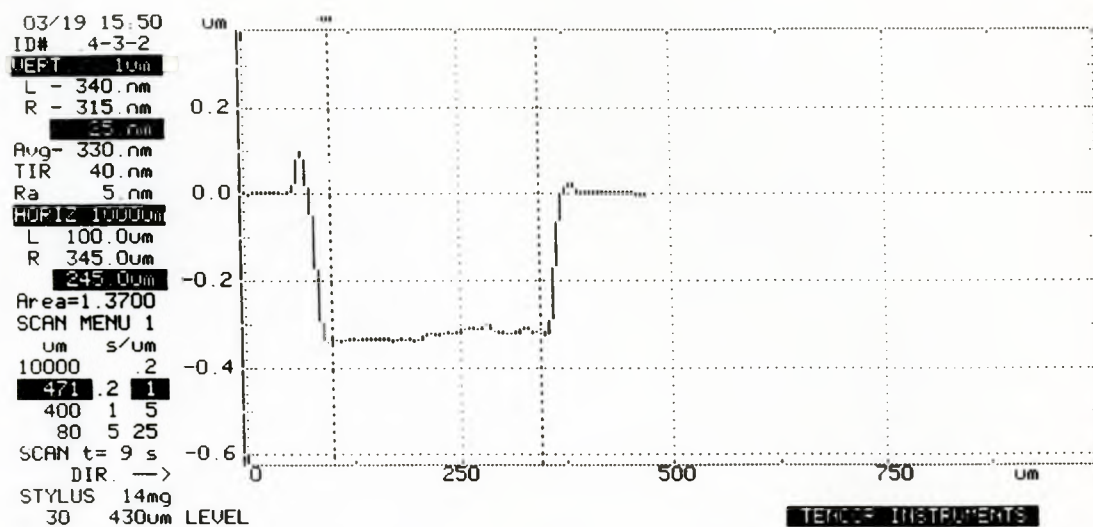


Figure 4.3a Surface profile of a hole made by two incident pulses at a fluence of 187 mJ/cm^2 .

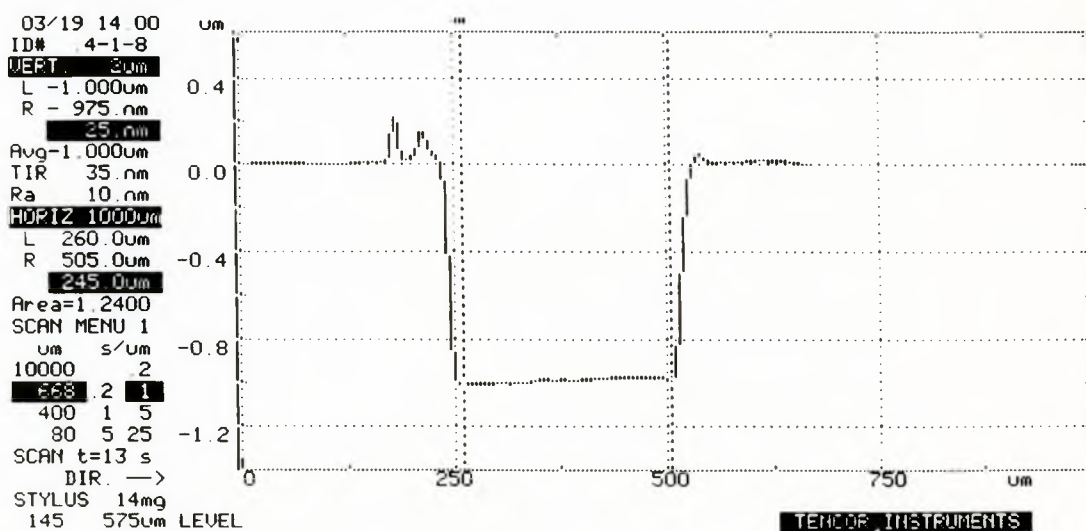


Figure 4.3b Surface profile of a hole made by eight incident pulses at a fluence of 187 mJ/cm^2 .

The surface shown is typical of ablated holes which only partially penetrate the layer. Figure 4.4c is a SEM image of a hole which completely penetrated the polyimide. It shows redeposited debris remaining on the silicon surface following ablation. Redeposited debris can be a problem since it forms a soot which does not absorb further UV radiation. As a result, the debris is not removed by subsequent laser pulses and further processing to remove it by other methods is undesirable. There is no evidence in the SEM images that the laser has ablated or damaged the silicon substrate. This was expected since the ablation threshold for silicon is much higher than for polyimide.

In Figure 4.5, the ablation rate is plotted as a function of the logarithm of the incident fluence. Equation 2.4 predicts a linear relationship with a slope of α^{-1} and an x-intercept given by the ablation threshold. A fit to the first eight data points gives a value of $67 \pm 6 \text{ mJ/cm}^2$ for the ablation threshold and an absorption coefficient of $(0.72 \pm 0.04) \times 10^5 \text{ cm}^{-1}$.

At fluences below 67 mJ/cm^2 , the ablation rate is negligible and fluences above this are required for significant material removal. Our experimental threshold value, along with those by other researchers, can be seen in Table 4.1. While our value is in reasonable agreement with the other values, there is some disagreement over the general shape of the ablation rate curve. Results by Brannon *et al*⁶ fit well to Equation 2.4 and the overall shape of their curve is in agreement with our results. However, results by Srinivasan *et al*⁷ did not fit well to Equation 2.4, especially at high incident fluences. Because we were unable to attain the high fluences used by Srinivasan, we could not



Figure 4.4a SEM image of the polyimide surface prior to irradiation.



Figure 4.4b SEM image of the bottom of a hole created by four pulses at a fluence of 187 mJ/cm^2 .

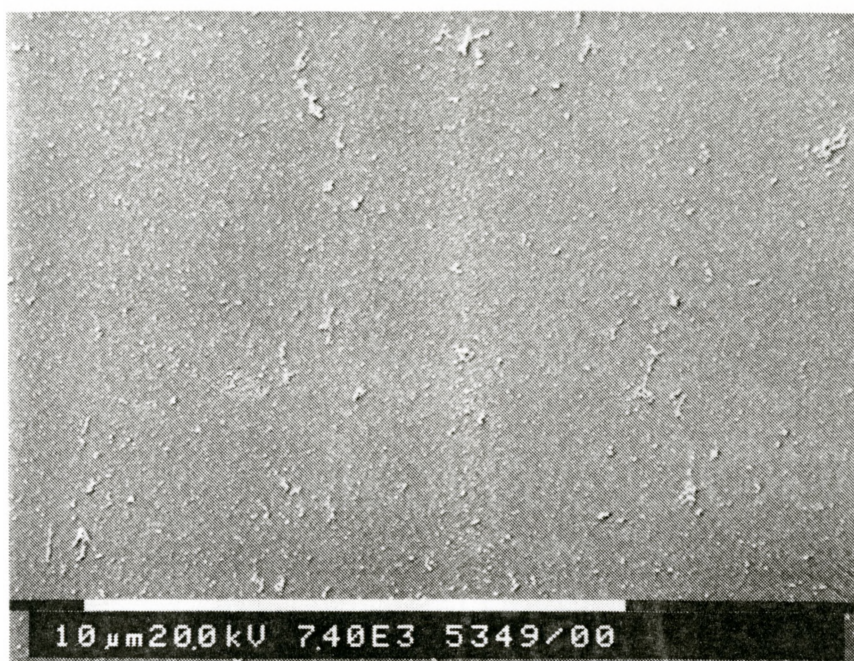


Figure 4.4c SEM image of the underlying silicon surface following ablation of the polyimide layer.

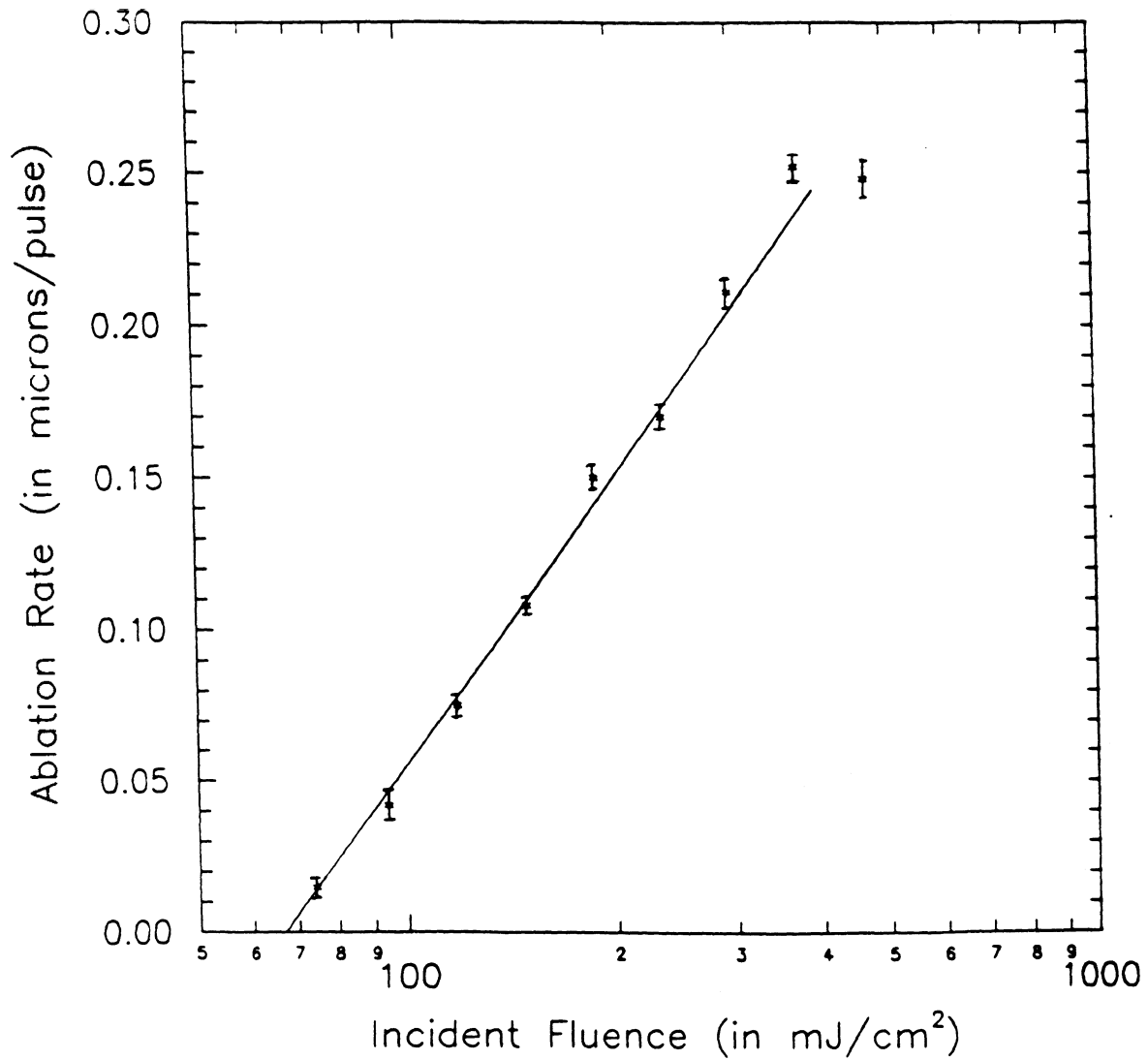


Figure 4.5 The ablation rate of polyimide versus the logarithm of the incident fluence. The x-intercept value of 67 mJ/cm² is the ablation threshold fluence.

Ablation Threshold (in mJ/cm ²)	Absorption Coefficient (units of 10 ⁵ cm ⁻¹)	Source
45	0.8	Dyer ¹
50	---	Singleton ¹⁸
60	---	Andrews ³
70	0.9	Brannon ⁶
100	---	Srinivasan ²⁷
67 ± 6	0.72 ± 0.04	Our value

Table 4.1 Experimental values for the ablation threshold and the absorption coefficient of polyimide.

examine the ablation process in this regime.

An estimation of the error in our measurements was determined in the following manner. A least squares fitting routine was used to determine the ablation rate from graphs of the ablated depth versus number of pulses (see Appendix A). In addition, the standard deviation (σ) of the slope was also calculated. Thus, for a given fluence, we were able to obtain both the ablation rate and its associated error. Since Figure 4.5 is a plot of the ablation rate as a function of fluence, the value of σ for each fluence is equal to the length of the error bars about that point. Although the amount of error is unique to each data point, experiments performed at higher fluences have larger errors. At these fluences the trials consisted of only a few pulses, whereas the lower fluence trials required many pulses to complete. Since the power output of the laser fluctuates, trials performed with few pulses have a greater chance of deviation than multiple pulse trials. Closer inspection of the graphs in Appendix A reveals that the value of the x-intercept is always positive. Although the x-intercept falls within experimental error of the origin in most cases, it is difficult to dismiss the fact that it is always positive as purely coincidental. The reason for this effect is unknown, but is most likely associated with a slight change in the polyimide's properties near the surface of the layer.

As previously mentioned (see section 2.1.2), the accepted low intensity value for the absorption coefficient is $1 \times 10^5 \text{ cm}^{-1}$ while our measured value was $(0.72 \pm 0.04) \times 10^5 \text{ cm}^{-1}$. This indicates that the incident pulse penetrates further into the polyimide than was expected. The reason for the difference between our value and the accepted

low intensity value is not certain, but it is likely due to saturation of the absorption. At a fluence of 300 mJ/cm^2 , the number of absorbed photons per monomer of polyimide could be as many as nine⁷, so saturation is possible.

4.2 REMOVAL AND DAMAGE OF ALUMINUM FILMS

A summary of results for processing aluminum on polyimide can be seen in Figure 4.6. The cracking threshold and the single shot removal (S.S.R.) threshold values for various aluminum film thicknesses are shown. Superimposed is the ablation rate of polyimide taken from Figure 4.5. As defined in section 3.4.2, the cracking threshold is the maximum fluence incident upon the aluminum surface for 1000 pulses without visible cracking occurring. Analysis of Figure 4.6 reveals several results. The cracking thresholds for the 50 nm and 235 nm thick aluminum layers are 26 mJ/cm^2 and 41 mJ/cm^2 respectively. Since these values are less than the polyimide ablation threshold, it would be impossible to ablate polyimide without damaging these aluminum layers if they were exposed to the same incident pulse. This would not be the case for the 470 nm and 1000 nm thick aluminum layers since their cracking threshold is larger than the polyimide ablation threshold. The S.S.R. threshold of the aluminum layers was typically 3 to 5 times larger than their respective cracking thresholds, and in all cases was larger than the polyimide ablation threshold. The removal threshold for the 1000 nm layer could not be determined because it was larger than the maximum attainable fluence of our system. Numerical values for the cracking and removal thresholds which were

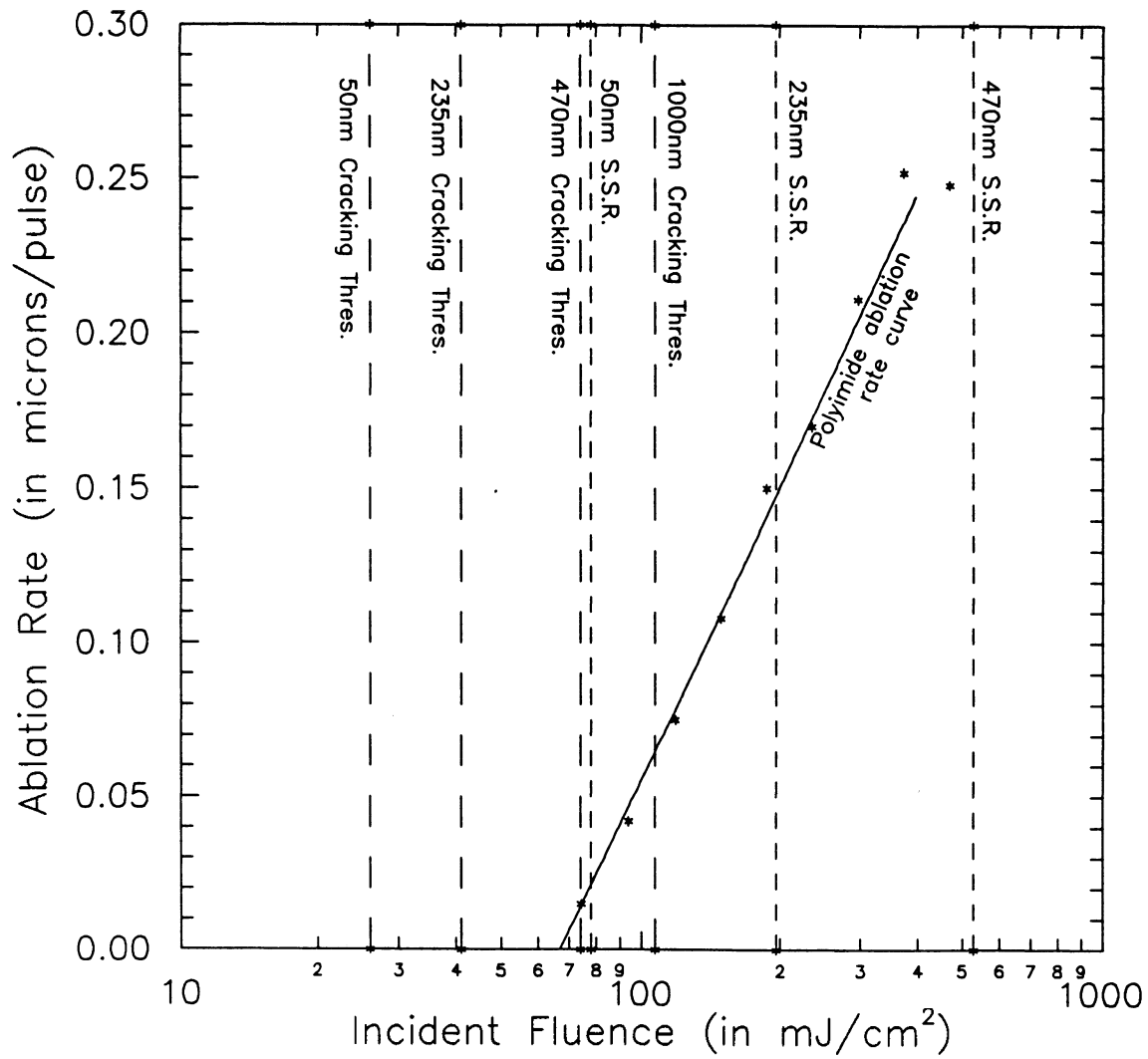


Figure 4.6 Cracking and S.S.R. threshold fluences for various thicknesses of aluminum with the polyimide ablation rate superimposed.

measured can be seen in Table 4.2.

In addition to determining the value of the S.S.R. threshold for a given aluminum film, we also wanted to examine the quality of the hole as a function of the incident fluence. A 235 nm thick aluminum layer deposited on polyimide was examined. The first hole was made by a single pulse at a fluence of 650 mJ/cm^2 and can be seen in Figure 4.7a. We notice that the edge quality of the hole is poor, since molten aluminum has splattered back onto the surrounding aluminum. This is more evident in Figure 4.7b, which is a SEM image of the edge of the hole. As calculated in Appendix B, the temperature rise in the irradiated area due to this pulse is approximately 890°C . Since the melting point of aluminum is 660°C ²⁶, it is likely that the aluminum is melting. In addition to poor edge quality, the surface morphology of the bottom of the hole is also poor. Further inspection of Figure 4.7a suggests that possible damage to the surface of the underlying polyimide may have occurred during removal. Figure 4.7c is a magnification of this damaged region. It appears as though the fluence of the incident pulse was large enough to cause some thermal degradation of the polyimide layer. Figure 4.7d is a SEM image showing sub-micron size spheres which are randomly scattered on the surface of the underlying polyimide. The composition of these spheres was determined to be aluminum using Energy Dispersive X-ray Spectroscopy (EDXS). The plot of the EDXS scan can be seen in Figure 4.8. The strong silicon peak in the EDXS spectrum is due to the background reading from the underlying silicon substrate. The shape of the aluminum fragments suggests that they were formed during the removal

Film Thickness (in nm)	Cracking Threshold (in mJ/cm ²)	S.S.R. Threshold (in mJ/cm ²)
50	26	78
235	41	196
470	74	528
1000	107	---

Table 4.2 Removal and cracking thresholds for various thicknesses of aluminum.

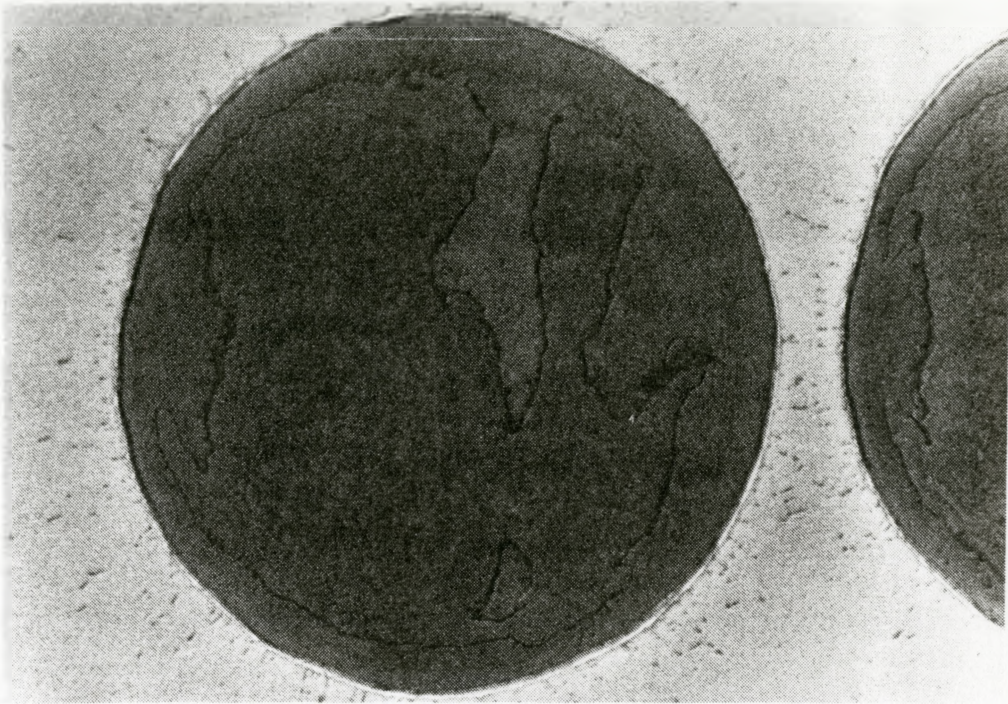


Figure 4.7a Photograph of a hole produced in a 235 nm thick aluminum layer by a single incident pulse at a fluence of 650 mJ/cm^2 .

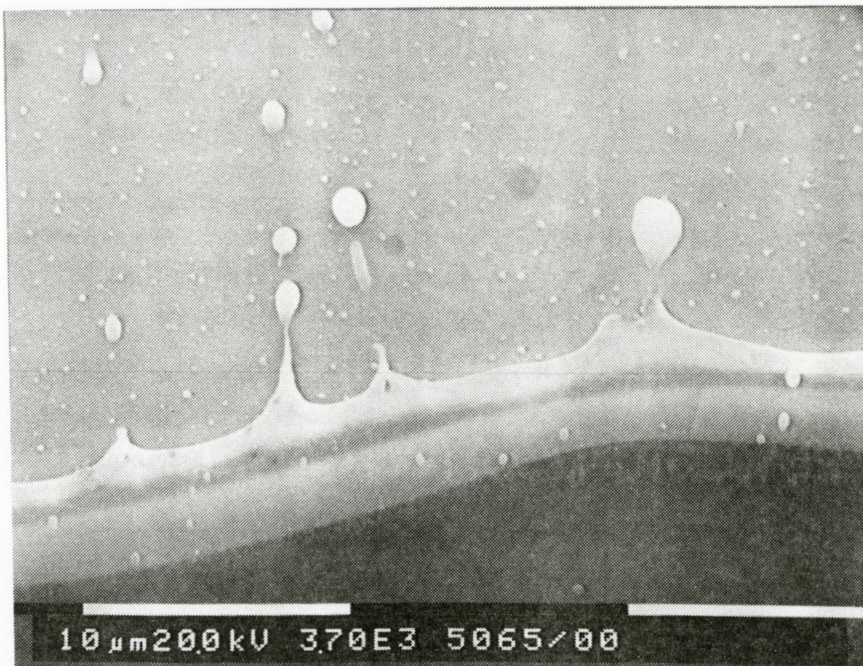


Figure 4.7b SEM image showing the edge quality of the hole in Figure 4.7a.

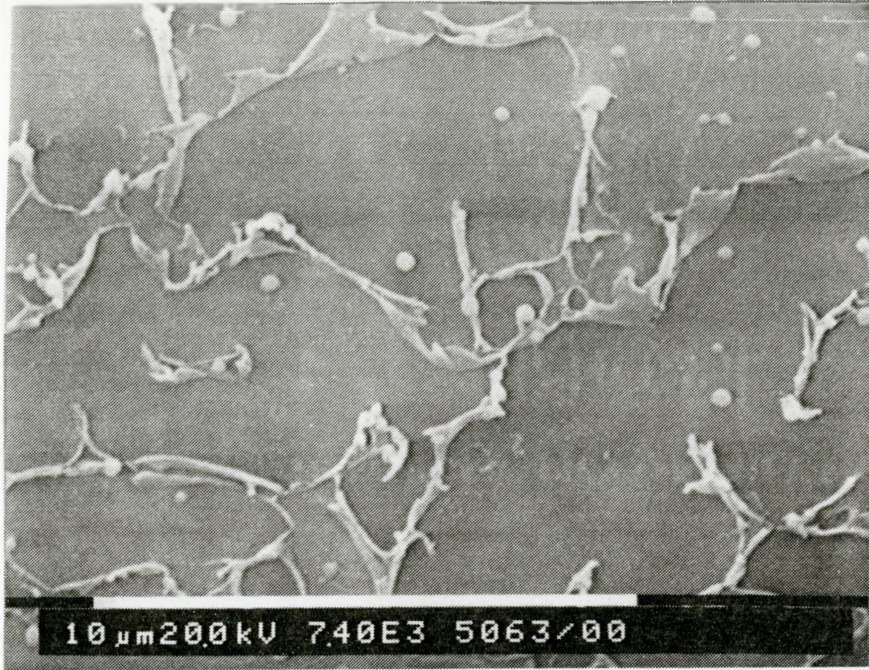


Figure 4.7c SEM image of the damaged region of the hole shown in Figure 4.7a.

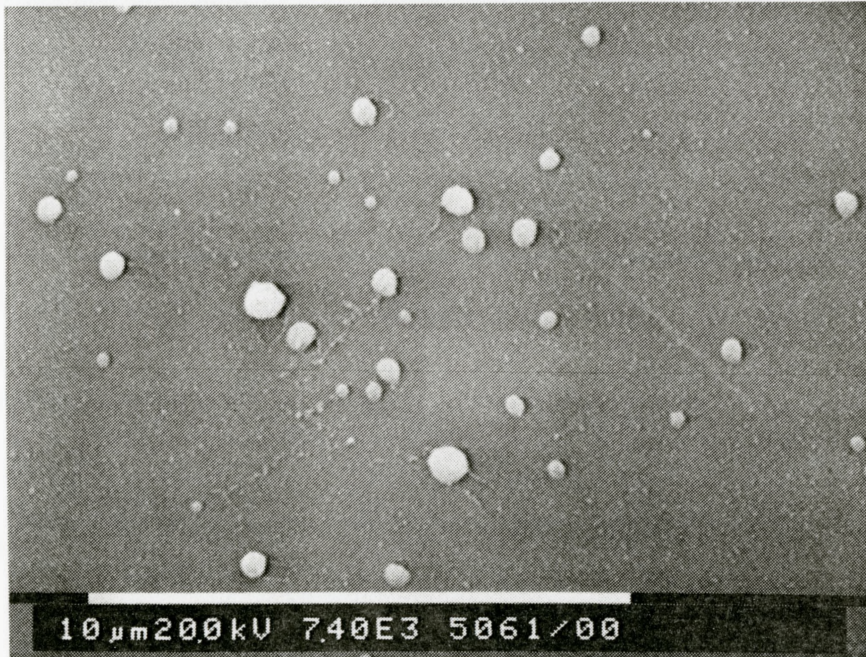


Figure 4.7d SEM image of debris at the bottom of the hole shown in Figure 4.7a.

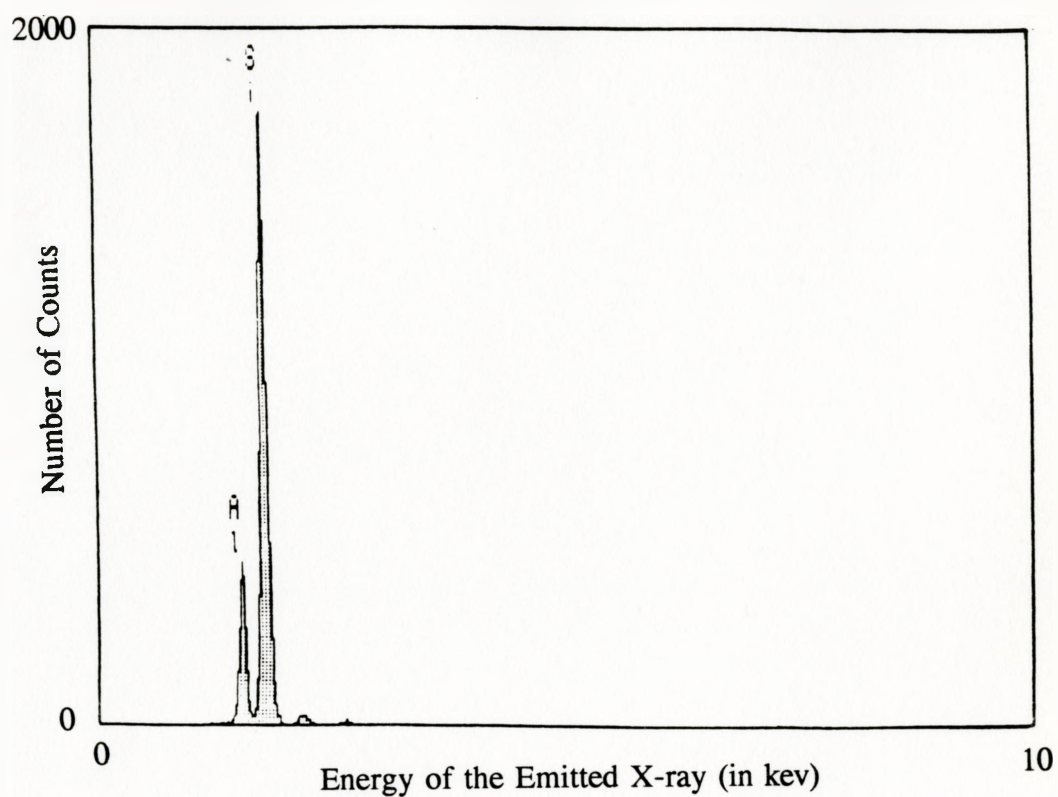


Figure 4.8 EDXS scan showing the composition of the debris at the bottom of the hole shown in Figure 4.7a. The peak indicating the presence of aluminum is located on the extreme left.

of the aluminum layer and were redeposited at the bottom of the hole.

At lower fluences, the quality of the hole improves. Figure 4.9a shows a hole produced at a fluence of 326 mJ/cm^2 . Since a single pulse at this fluence will produce a temperature rise of approximately 445°C , we expect that the melting of aluminum observed at higher fluences will no longer occur. From this photograph, it appears as though the underlying polyimide is undamaged. Closer inspection with the electron microscope confirmed this. The SEM image in Figure 4.9b shows that the same type of damage which occurred to the polyimide at 650 mJ/cm^2 (Figure 4.7c) did not occur at 326 mJ/cm^2 . In addition, the amount of aluminum redeposited on the polyimide is significantly reduced. Figure 4.9c shows that the edge quality of this hole has also improved. The splattering of molten aluminum previously observed (see Figure 4.7c) is absent and the width of the edge between the hole and the surrounding aluminum is reduced. The debris in the top right portion of the photograph is most likely redeposited aluminum, although this could not be verified by EDXS due to the strong background aluminum signal.

At yet lower fluences, the quality of the hole deteriorates. Figure 4.10a is a photograph of a hole produced at a fluence of 205 mJ/cm^2 , which is just above the S.S.R. threshold of the material. As can be seen in Figure 4.10b, the aluminum layer around the perimeter of the hole is cracked, wrinkled and uneven. It is important to note that the magnification of this SEM image is less than in Figure 4.9c, so the edge quality is worse than it appears.

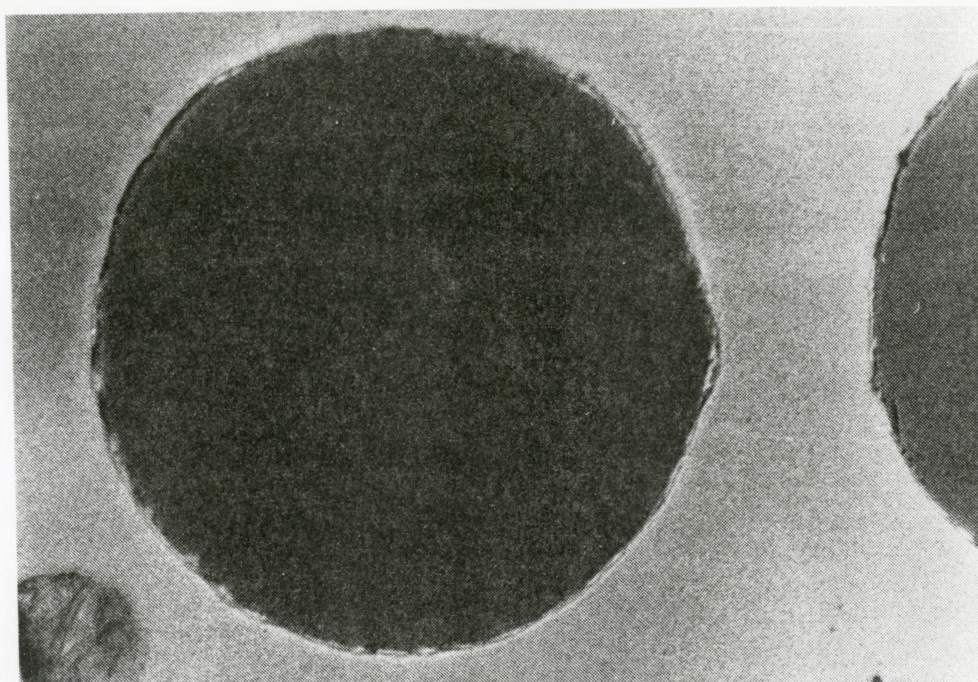


Figure 4.9a Photograph of a hole produced in a 235 nm thick aluminum layer by a single incident pulse at a fluence of 326 mJ/cm².

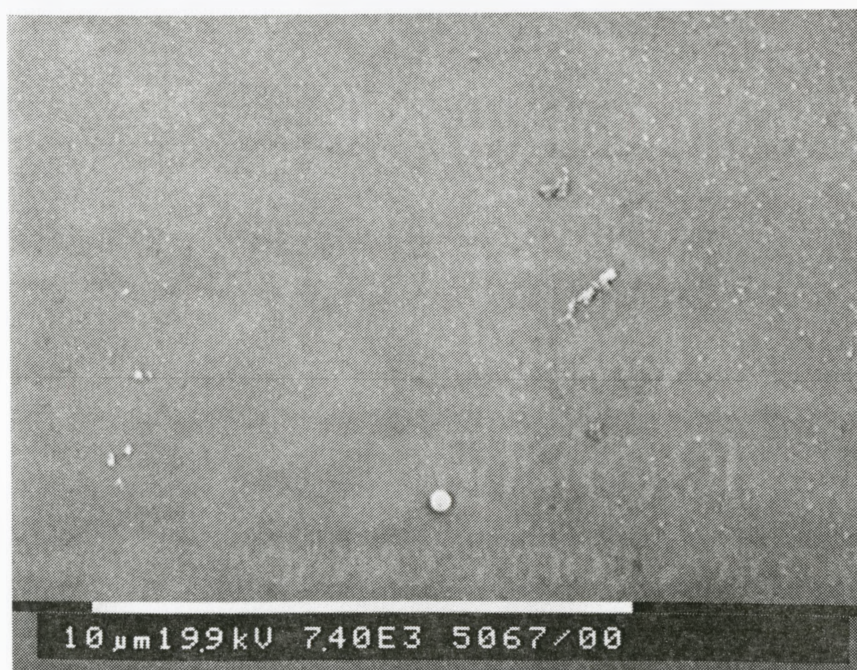


Figure 4.9b SEM image of the bottom of the hole shown in Figure 4.9a.



Figure 4.9c SEM image showing the edge quality of the hole in Figure 4.9a.

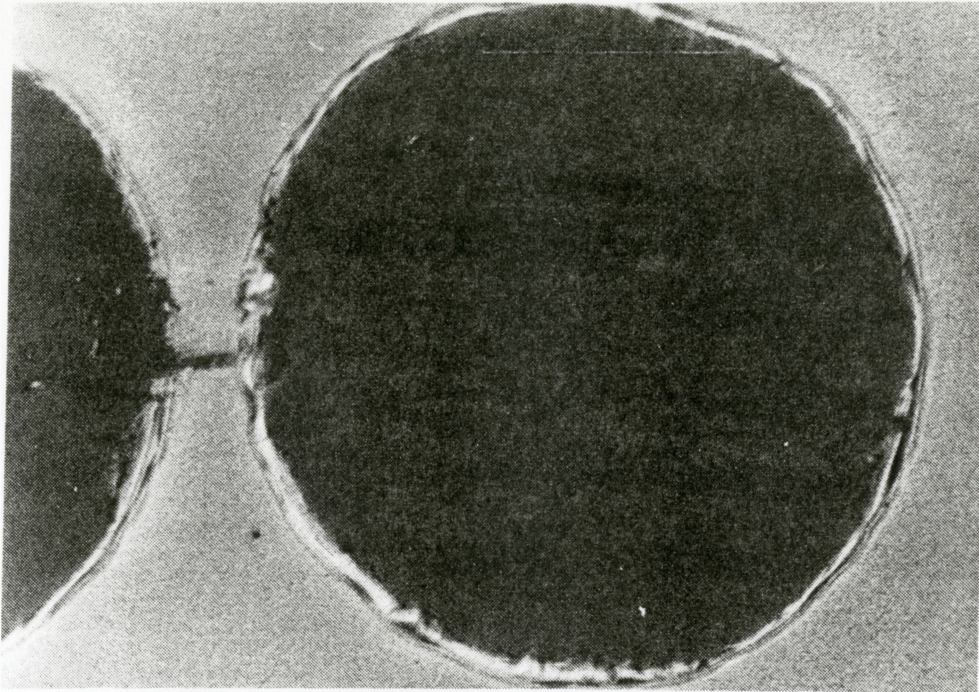


Figure 4.10a Photograph of a hole produced in a 235 nm thick aluminum layer by a single incident pulse whose fluence (205 mJ/cm^2) is just above the S.S.R. threshold.



Figure 4.10b SEM image showing the edge quality of the hole in Figure 4.10a.

At fluences slightly below the S.S.R. threshold, removal of the aluminum layer ceases and only heavy damage occurs. In Figure 4.11a, we see a section of the aluminum layer which has been exposed to a single pulse at a fluence of 163 mJ/cm^2 . The central portion of the photograph shows the irradiated zone while to the left we see part of a hole from a previous trial. There is intense cracking and partial film removal in the top portion of the irradiated area. SEM images of this heavily damaged region can be seen in Figures 4.11b, 4.11c and 4.11d. Figure 4.11b is a magnification of Figure 4.11a showing cracking of the aluminum layer. The fluence of the incident pulse was too low to completely remove the film, so most of the aluminum was left behind. There are also dark spots on the surface of the aluminum. These spots were present in only a small section of the entire irradiated area and were not observed in any other SEM images. This indicates that the incident laser pulse did not create the spots, although the reason for their existence is unknown. Figure 4.11c shows a region of the sample where the aluminum has been peeled back rather than removed. Cracking and wrinkling of the aluminum surrounding this region has also occurred. This is most likely due to thermal effects. Figure 4.11d is a magnification of the previous photograph showing the debris remaining on the polyimide surface after the aluminum has been peeled back. The physical appearance of the debris indicates that it is most likely polyimide rather than redeposited aluminum. This conclusion was supported by the EDXS analysis seen in Figure 4.12, which shows that the debris does not contain aluminum.

The cracking thresholds plotted in Figure 4.6 are the thresholds for 1000 laser

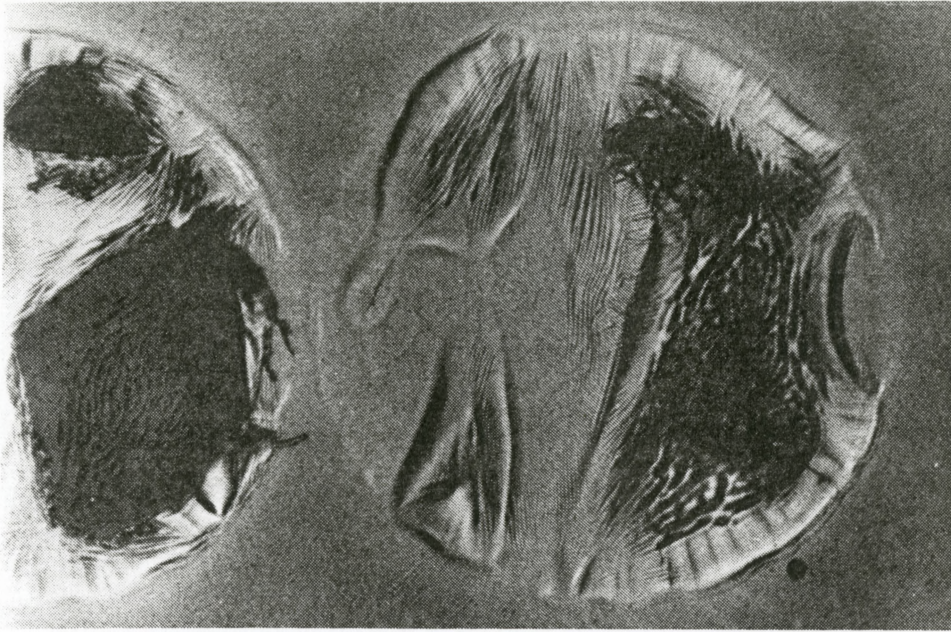


Figure 4.11a Photograph showing heavy damage to a 235 nm thick aluminum layer caused by a single incident pulse at a fluence (163 mJ/cm^2) just below the S.S.R. threshold.

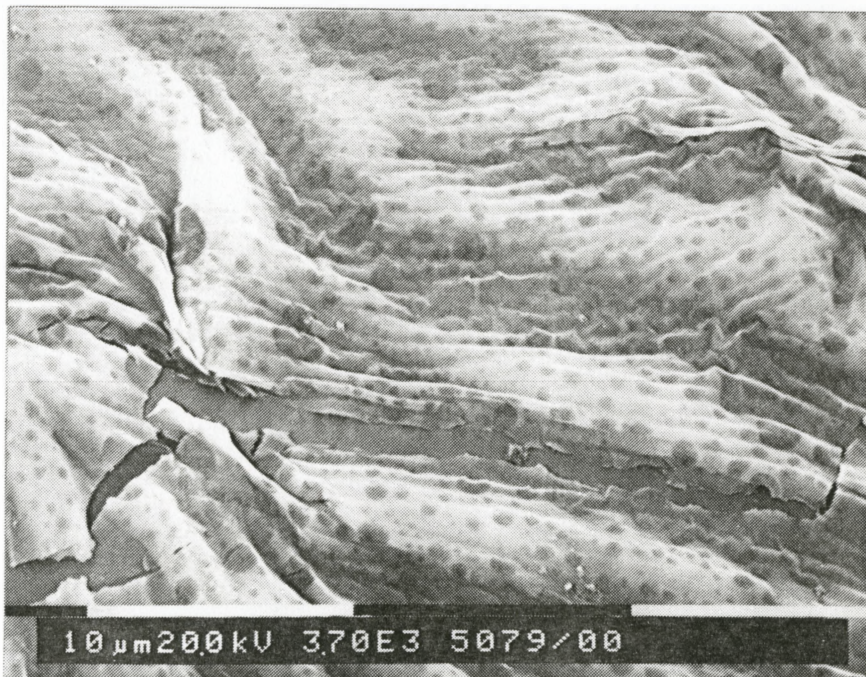


Figure 4.11b SEM image showing cracking and partial removal of the aluminum in the damaged region of Figure 4.11a.

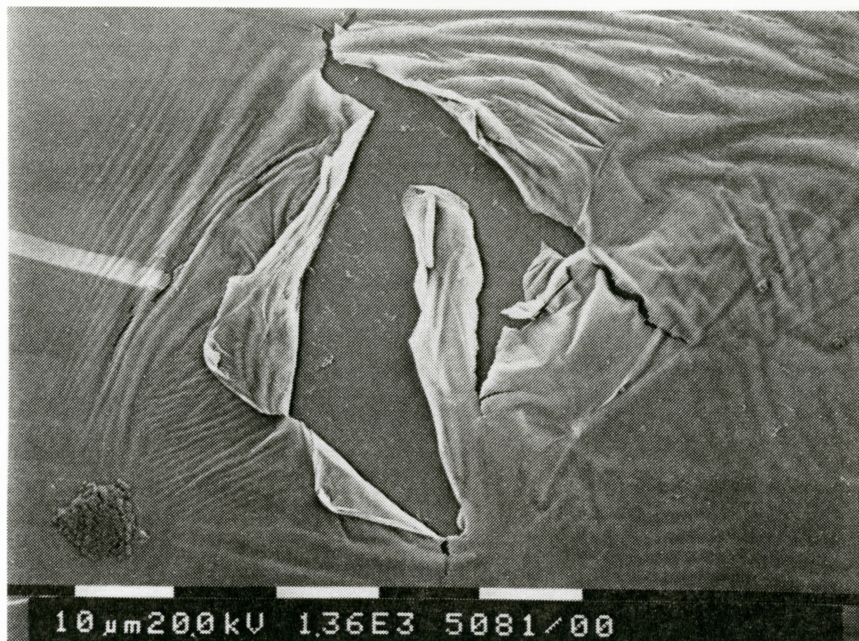


Figure 4.11c SEM image showing a region where the aluminum layer has been peeled back by the incident pulse.

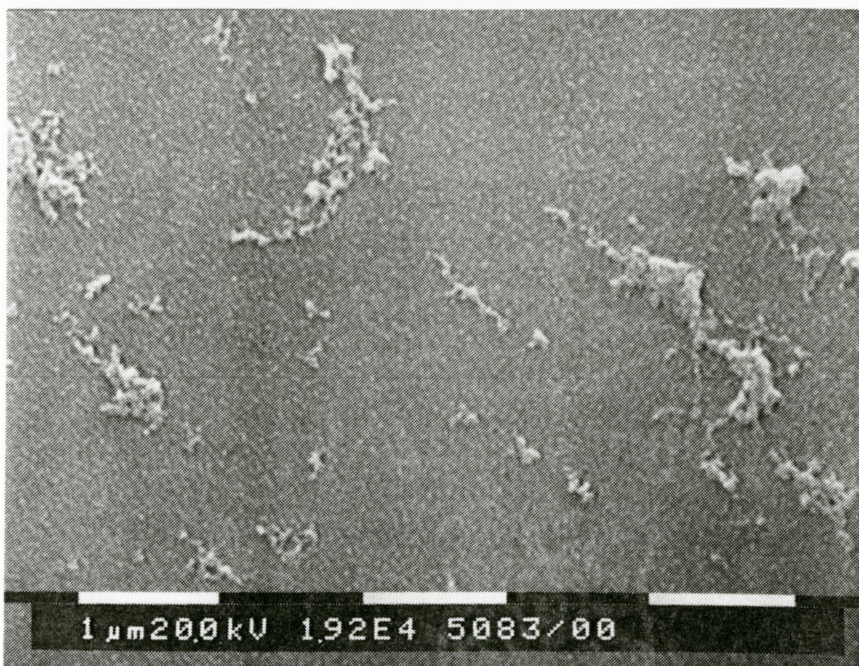


Figure 4.11d Magnification of Figure 4.11c, showing debris on the surface of the underlying polyimide layer.

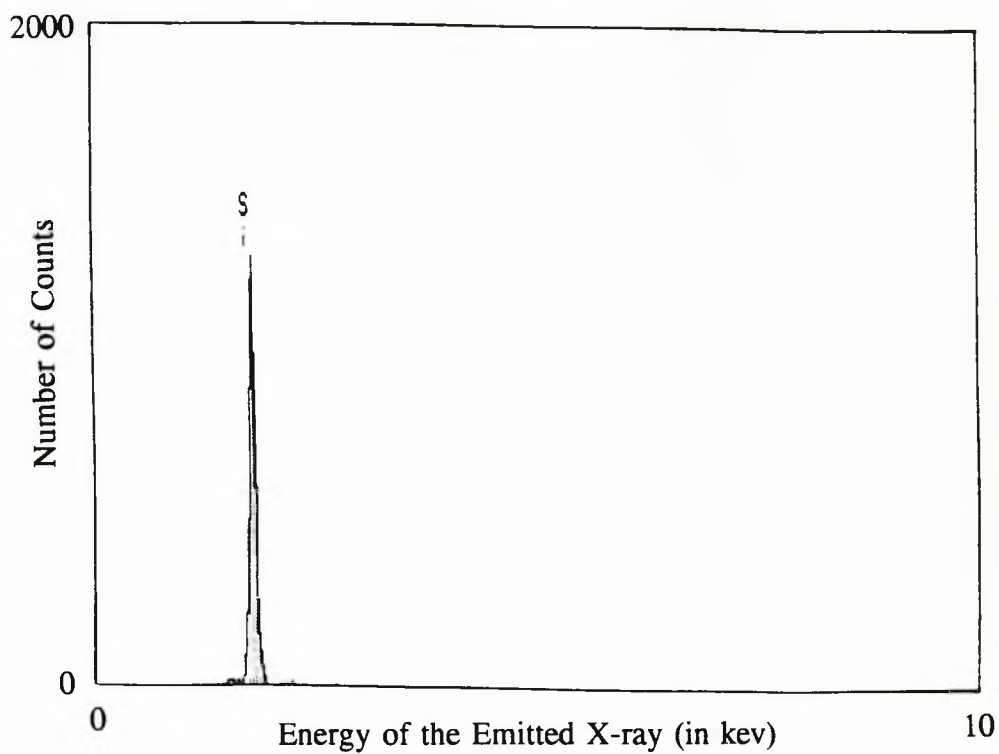


Figure 4.12 EDXS scan of the composition of the debris remaining on the underlying polyimide surface after the aluminum layer has been peeled back. The peak indicating the presence of aluminum (see Figure 4.8) is not present in this scan.

pulses. At slightly higher fluences, cracking will occur after a fewer number of pulses. Figure 4.13 shows the number of pulses required to initiate cracking as a function of the incident fluence, with each curve on the graph corresponding to a different aluminum layer thickness. The most obvious feature of this plot is that thicker aluminum layers are less sensitive to small changes in fluence and are therefore more resilient to cracking. For the 50 nm aluminum layer, the cracking threshold was 26 mJ/cm^2 for 1000 laser pulses. If the fluence is raised to 33 mJ/cm^2 , then it only requires 10 laser pulses to cause similar damage. The damage threshold for the 1000 nm aluminum layer was 107 mJ/cm^2 , which is approximately four times larger than the threshold for the 50 nm layer. If we wanted to do similar damage to this layer in only 10 pulses, then the incident fluence would have to be raised to approximately 200 mJ/cm^2 . The damage thresholds for various film thicknesses can be seen in Table 4.3.

Figure 4.14a shows cracking of a 470 nm thick layer by two laser pulses at a fluence of 265 mJ/cm^2 . We notice that the cracking is uniform over the entire irradiated region and neither removal nor peeling back of the aluminum has occurred. Figure 4.14b shows the effect of ten similar laser pulses on the same layer. Both the number and the density of cracks has increased. In addition, partial removal and peeling back of the aluminum layer has occurred in parts of the irradiated zone. The size and location of this partially removed region was inconsistent from trial to trial. If further pulses were applied, the size of this region eventually increased to cover the entire irradiated area. These results indicate why aluminum is more effectively removed by a single shot

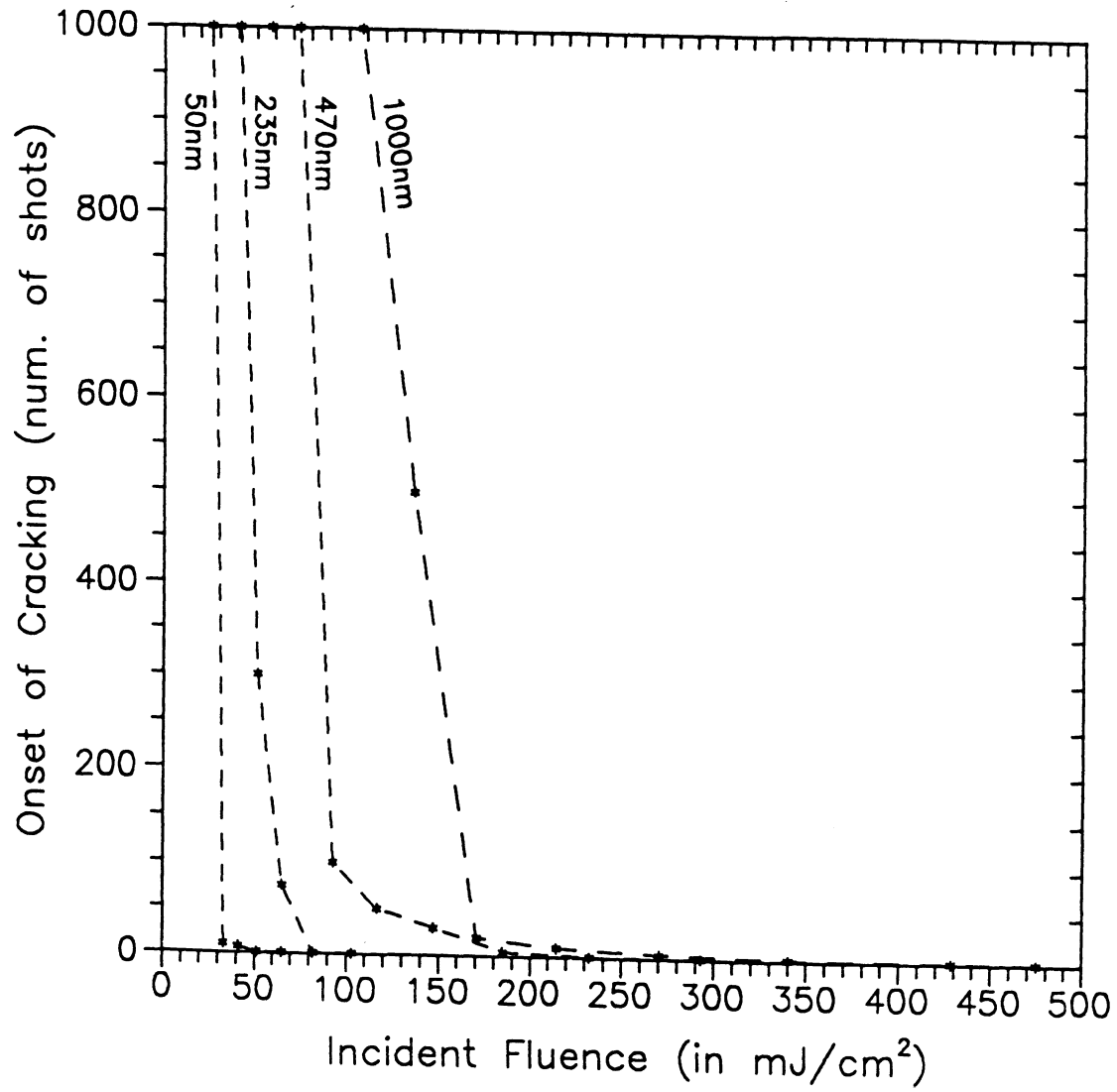


Figure 4.13 The onset of cracking as a function of incident fluence for various thicknesses of aluminum.

Film Thickness (in nm)	Incident Fluence (in mJ/cm ²)	Number of pulses to cause damage.
50	26	1000
	33	10
	41	7
	51	1
	65	1
235	41	1000
	51	300
	65	75
	82	1
	103	1
470	58	1000
	74	1000
	93	100
	116	50
	147	30
	185	5
	233	1
	293	1
1000	107	1000
	136	500
	170	20
	215	10
	270	5
	340	2
	428	1
	475	1

Table 4.3 The number of incident pulses required to cause damage at a given fluence for various aluminum layer thicknesses.

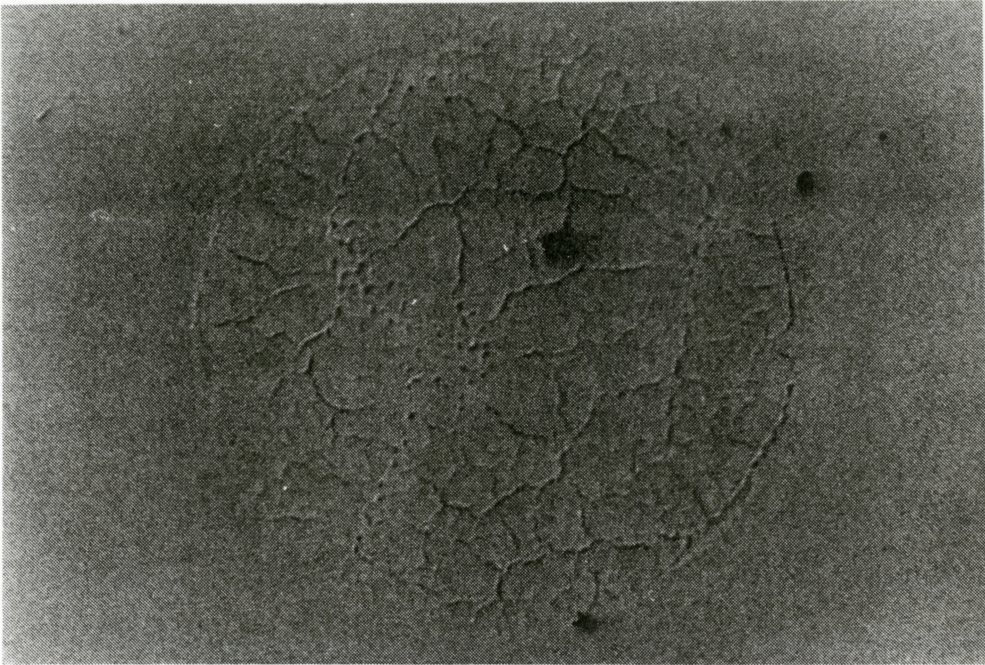


Figure 4.14a Photograph showing cracking of a 470 nm thick aluminum layer caused by two incident pulses at a fluence of 265 mJ/cm².

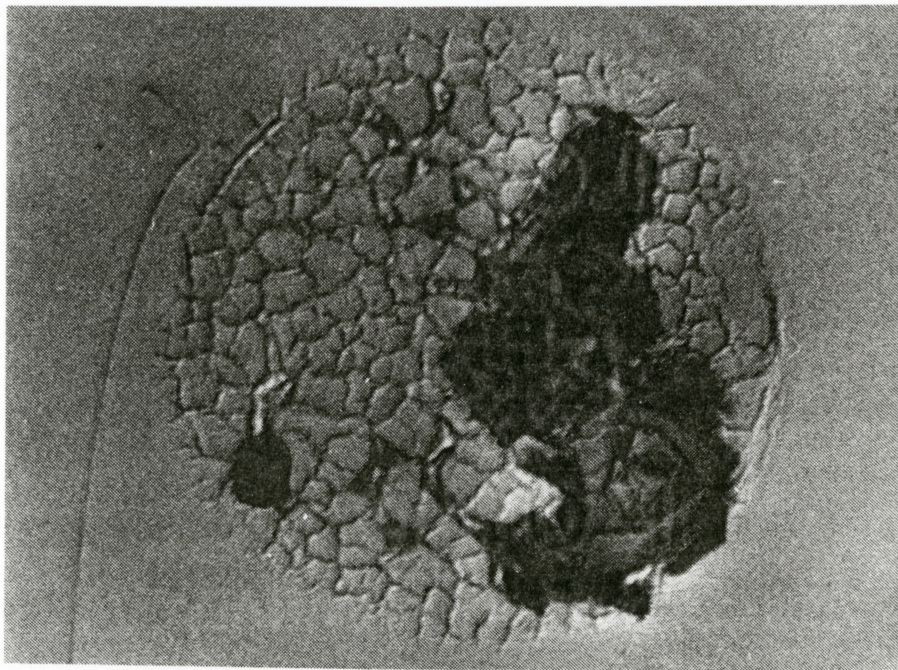


Figure 4.14b Photograph showing cracking of the same layer as above, but caused by ten incident pulses at a fluence of 265 mJ/cm².

rather than a multiple shot technique. There were two basic problems associated with a lower fluence multiple shot removal technique. First, the edge quality of the aluminum surrounding the irradiated region is poor since the aluminum tended to be peeled back rather than removed. Second, and more important, it was impossible to obtain an undamaged surface on the underlying polyimide layer. Since the aluminum layer was removed in multiple shots rather than a single one, regions of the underlying polyimide were directly exposed to incident pulses while others were not. The fluence of these pulses was sufficient to cause polyimide ablation, resulting in a polyimide surface profile which was dependent upon which areas of aluminum were removed first. By employing the single shot removal technique, the problems of the multiple shot technique could be averted. The higher fluences associated with S.S.R. resulted in improved edge quality and since removal occurred in a single pulse, the underlying polyimide was never directly exposed to an incident pulse.

The errors associated with the results for aluminum removal are difficult to quantify. Since the aluminum was removed by a single pulse, the error in the threshold S.S.R. value is equal to the difference in power transmission between successive neutral density filters. For example, removal of a 235 nm thick layer occurred at a fluence of 196 mJ/cm², but not at 155 mJ/cm². The actual S.S.R. value most likely lies between these two values, but we were unable to examine fluences in this range due to the lack of sensitive filters. The error associated with the cracking experiments was also difficult to quantify. Determination of the cracking threshold was subjective since it was done

by visual inspection. In addition, the error was dependent upon the number of incident pulses (and therefore the incident fluence). If cracking occurred after only a few pulses, then the associated error is smaller than if hundreds of pulses were required.

4.3 SELECTIVE ABLATION OF THE MULTILAYER

Once the fluences required for polyimide and aluminum removal were determined, the selective ablation of a polyimide-aluminum-polyimide multilayer was attempted. A starting fluence of approximately 190 mJ/cm^2 was selected because it provided a significant polyimide ablation rate. Ablation of the majority of the upper polyimide layer was carried out, but was stopped prior to complete penetration. The number of shots required to reach this point could easily be determined knowing the ablation rate and the polyimide thickness. If directly exposed to the underlying aluminum, the initial fluence was large enough to cause damage. In order to prevent this, the incident fluence was lowered to 98 mJ/cm^2 , which is still above the polyimide ablation threshold. As can be seen in Table 4.3, an aluminum layer approximately 470 nm in thickness can withstand between 1 and 5 pulses at a fluence of 190 mJ/cm^2 before the onset of damage. However, if the fluence is only 98 mJ/cm^2 , between 50 and 100 pulses are required to cause similar damage. The surface could therefore be exposed to several direct laser pulses in order to ablate the remainder of the polyimide without any risk of damage to the underlying aluminum. The ablation process was continued at this lower fluence until the polyimide was removed. The lower fluence could have been used to ablate through

the entire polyimide layer, but this would have required a far greater number of shots. Figures 4.15a and 4.15b are a photograph and a surface profile of this hole respectively. There is little debris on the surface of the aluminum, but redeposited debris is present on the surrounding polyimide near the edge of the hole. The type of damage present in Figures 4.14a or 4.14b does not appear in Figure 4.15a. Figure 4.15c is a SEM image of the bottom of this hole showing the aluminum surface subsequent to ablation, while Figure 4.15d shows an aluminum surface which has not been exposed to any laser light. In comparing the two figures, we notice that the same surface roughness is present prior to irradiation and so direct exposure to the incident pulses had no observable effect on the aluminum layer. Figure 4.15e shows debris on the polyimide surface surrounding the hole. This debris consists of ablated polyimide from the irradiated zone which has redeposited on this neighbouring surface.

The next stage of processing involved removing the polyimide and aluminum layers while stopping at the lower polyimide layer. The top polyimide layer was ablated using the same fluence and technique as described above. The removal of the aluminum layer was performed with a single laser pulse at the maximum fluence of 528 mJ/cm^2 . As mentioned in section 4.2, the S.S.R technique was found to produce the best quality hole. Figure 4.16a is a photograph of the hole while Figure 4.16b is its associated surface profile. The surface is smooth and flat indicating that the underlying polyimide had not been ablated. Figure 4.16c is a SEM magnification of this surface, showing damage to the polyimide. The incident pulse caused a temperature rise of approximately

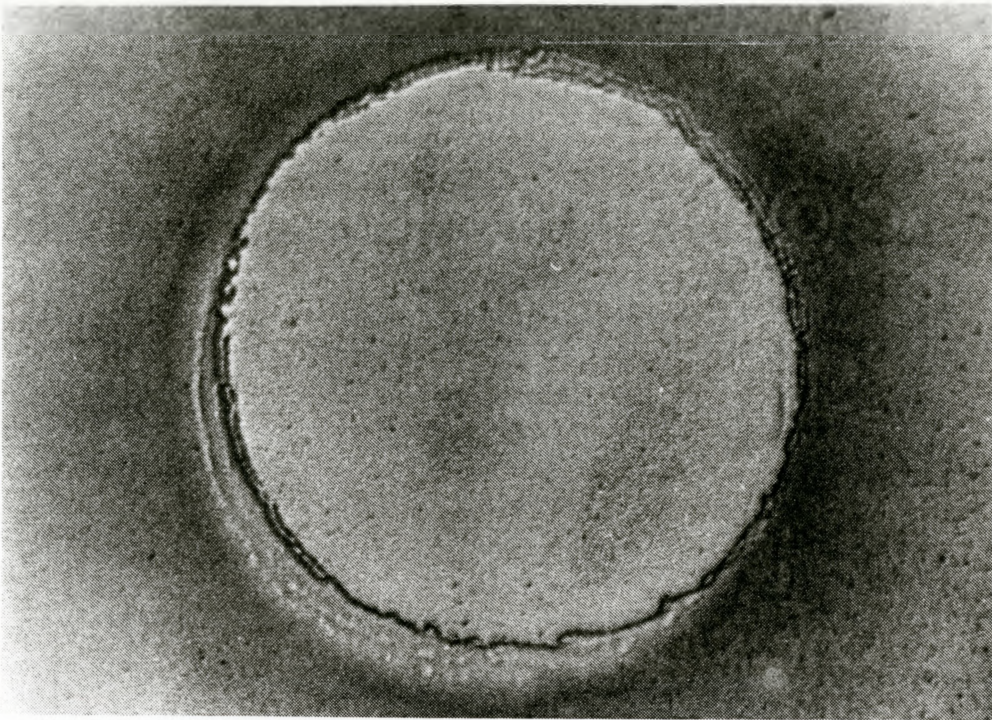


Figure 4.15a Photograph of a hole ablated through the upper polyimide layer of a multilayer.

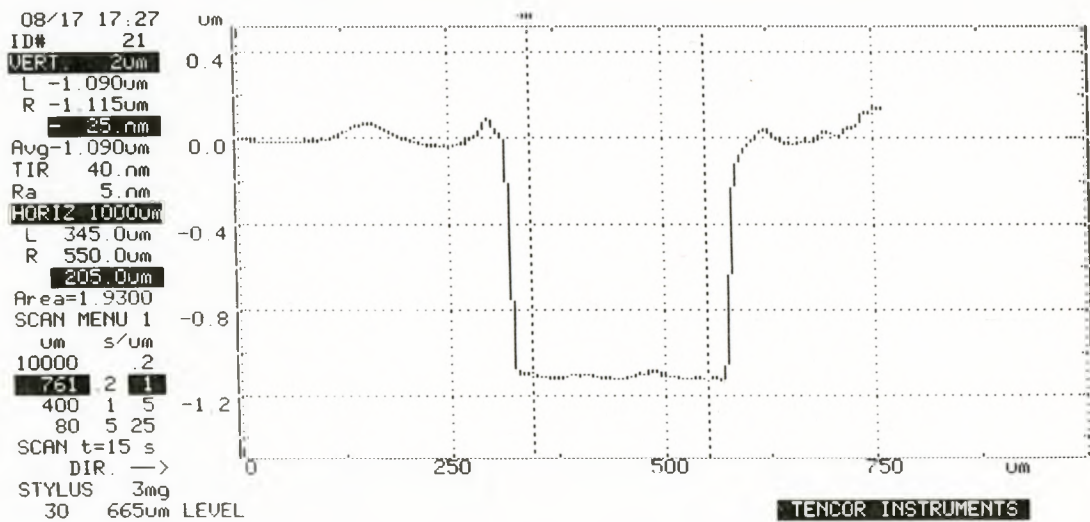


Figure 4.15b Surface profile of the above hole.



Figure 4.15c SEM image showing the bottom surface of the hole from Figure 4.15a.



Figure 4.15d SEM image showing the surface of a section of the aluminum layer which has not been exposed to laser light.



Figure 4.15e SEM image of debris surrounding the hole shown in Figure 4.15a.

360°C within the aluminum layer. It is unlikely that this temperature was high enough to damage the polyimide since it was shown earlier (see section 4.2) that the aluminum layer could be heated to 445°C without damaging the underlying polyimide. However, it is possible that the polyimide surface was inadvertently damaged in fabricating the multilayer. The edge quality of this hole (see Figure 4.16d) is poorer than the hole shown in Figure 4.9c. A possible reason for the mediocre edge quality is that the incident fluence was not high enough to produce a good edge. This situation is similar to that in Figures 4.10a and 4.10b, in which the fluence of the incident pulse was just above the S.S.R. threshold of the layer. Comparison of Figures 4.10b and 4.16d reveal that the edge quality of the holes is similar. Since we were already removing the aluminum at the maximum attainable fluence of our system, we were unable to determine if the edge quality would improve at higher fluences.

In order to penetrate through the entire multilayer, the technique of alternating between single shot removal of the aluminum and lower fluence multiple shot ablation of the polyimide was employed. Upon removal of the aluminum, the incident fluence was again lowered to 190 mJ/cm² and the polyimide layer was removed. The surface quality of the silicon following the polyimide ablation was good. Figure 4.17a is a surface profile of the silicon which shows that there is some debris remaining on the surface following ablation. This was confirmed by the SEM image seen in Figure 4.17b, which shows sub-micron fragments on the silicon. EDXS was performed on the fragments (see Figure 4.18) which indicated that they did not contain aluminum. It is

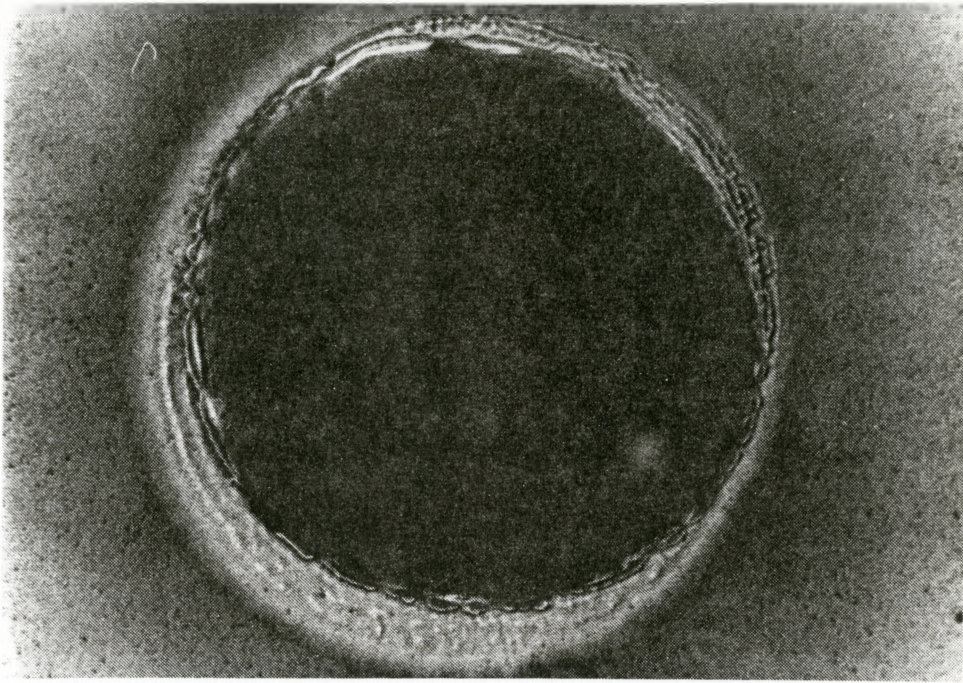


Figure 4.16a Photograph of a hole which penetrates through both the upper polyimide and aluminum layers.

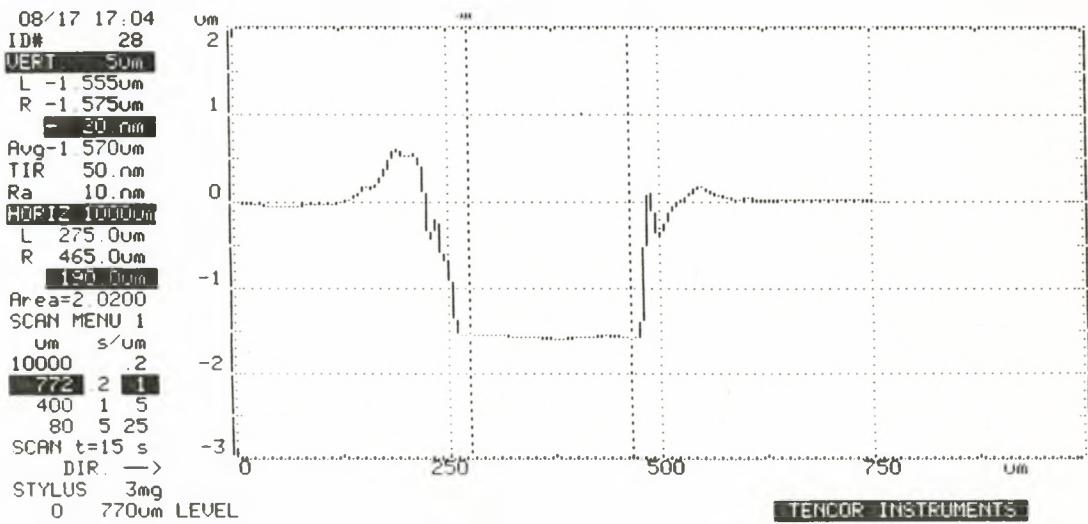


Figure 4.16b Surface profile of the above hole.



Figure 4.16c SEM image of the bottom of the hole shown in Figure 4.16a.



Figure 4.16d SEM image showing the edge quality of the hole in Figure 4.16a.

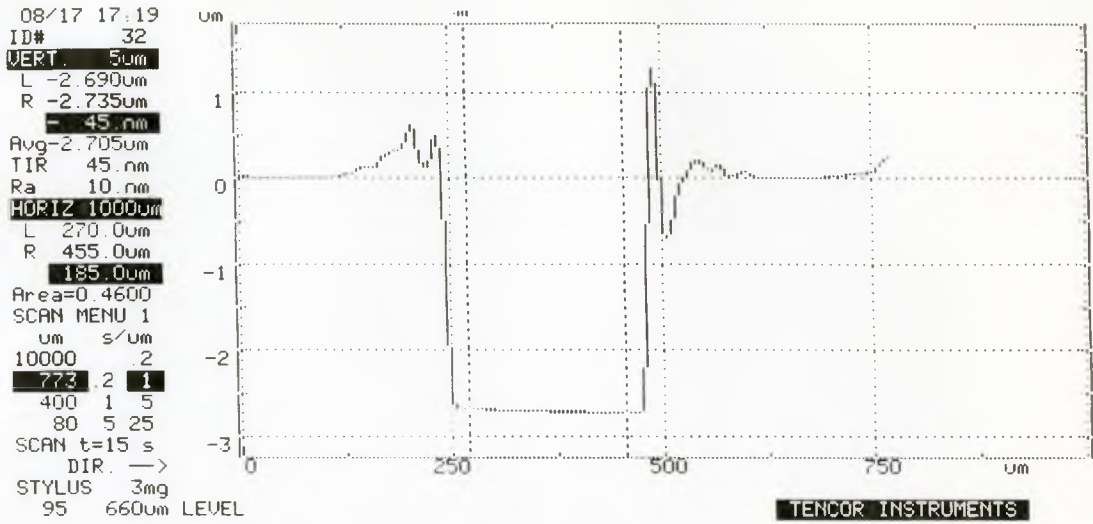


Figure 4.17a Surface profile of the silicon substrate following removal of the multilayer.



Figure 4.17b SEM image of the silicon surface following removal of the multilayer.

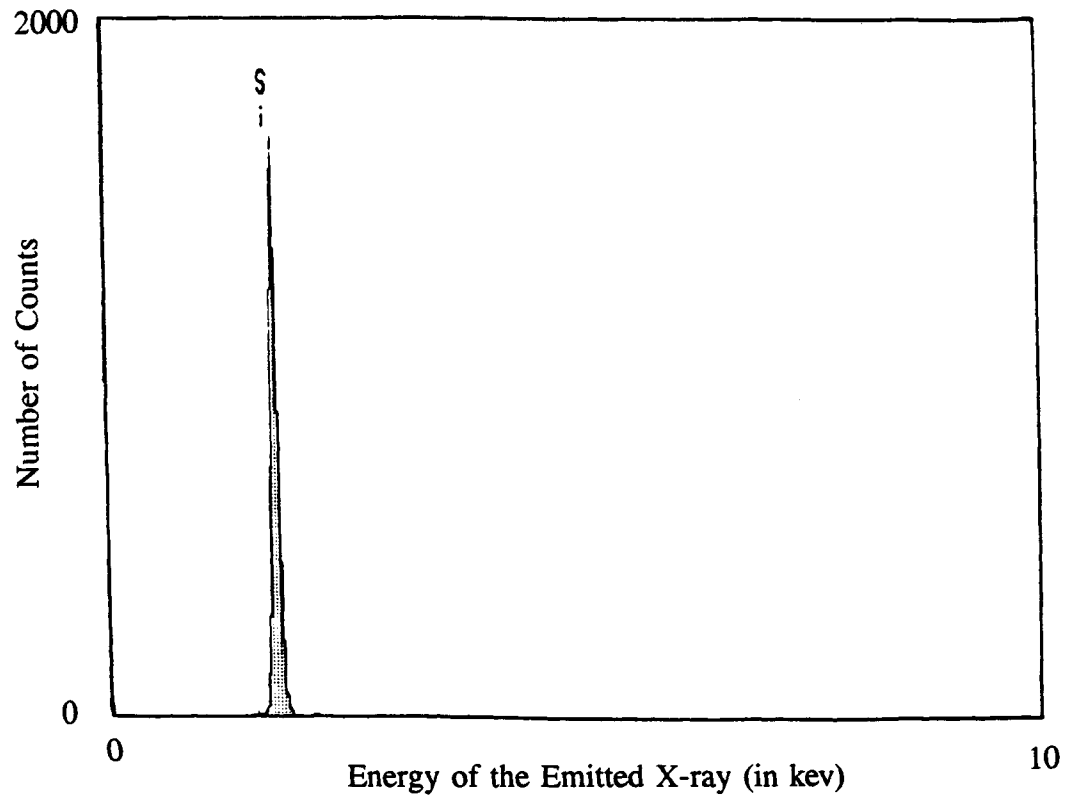


Figure 4.18 EDXS scan showing the composition of the debris remaining on the silicon surface after the multilayer has been removed. The peak indicating the presence of aluminum (see Figure 4.8) is not present.

likely that these fragments are composed of redeposited polyimide. The SEM images of the surface do not reveal any cracking, melting or ablation of the silicon. All of these results agree with those obtained in section 4.1. As in SEM images of previous holes, there is once again a great deal of redeposited debris around the perimeter of the hole.

An alternate method for removing the entire multilayer is to select a fluence larger than the polyimide and aluminum removal thresholds, but less than the damage threshold of silicon. A sufficient number of pulses are applied until the multilayer is penetrated. Due to the relatively large value of the silicon ablation threshold, ablation ceases upon reaching the silicon surface. This method is both simpler and quicker than the alternating fluence method, but it was found that the edge quality of the hole was not as good. The removal of the aluminum layer was invariably hampered by the fact that a clean, polyimide-free aluminum surface was not present to permit good S.S.R. of the aluminum. The aluminum tended to peel and blister rather than be cleanly removed, resulting in a poorly defined edge.

4.4 INCUBATION OF POLYIMIDE

As mentioned in section 3.4.5, the free standing polyimide film was exposed to low levels of laser light to determine if incubation was occurring. Incubation involves chemical changes in the material which should be observed as a change in the infrared transmission of the film. These chemical changes may also affect the ultraviolet absorption characteristics of polyimide, and could then be detected by examining its

ultraviolet transmission spectrum. Figures 4.19a and 4.19b show transmission through the film as a function of the incident wavelength before and after irradiation respectively. Polyimide absorbs strongly in the ultraviolet and so very little light is transmitted. If significant incubation was occurring, then the absorption coefficient would change, resulting in a change in the amount of transmission through the film. Comparison of the two figures indicates that there is no change in the spectrum following irradiation. From these figures we cannot ascertain whether or not there are chemical changes, only that there is no significant change in the absorption coefficient.

If low level irradiation selectively breaks chemical bonds in the material, then the number of these bonds present in the film would decrease as a function of irradiation. Figure 4.20a shows the infrared transmission of the film as a function of wavelength prior to irradiation. If particular bonds were being broken during irradiation, then the absorption peaks in the transmission spectrum associated with these bonds would be reduced. By examining the transmission of the film before and after irradiation, we were able to determine which bonds if any, were being severed. Figure 4.20b shows the infrared transmission spectrum of the film following irradiation by a total of 2000 laser pulses at a fluence of 28 mJ/cm^2 , which corresponds to an average dose of approximately 350 photons per molecule within the film. This dose was enough to sufficiently irradiate the film. From Figure 4.20b we can conclude two things. The fact that none of the peaks in the spectrum changed in size indicated that the relative numbers of these bonds were unchanged. In addition, no new peaks appeared in the spectrum, indicating that the

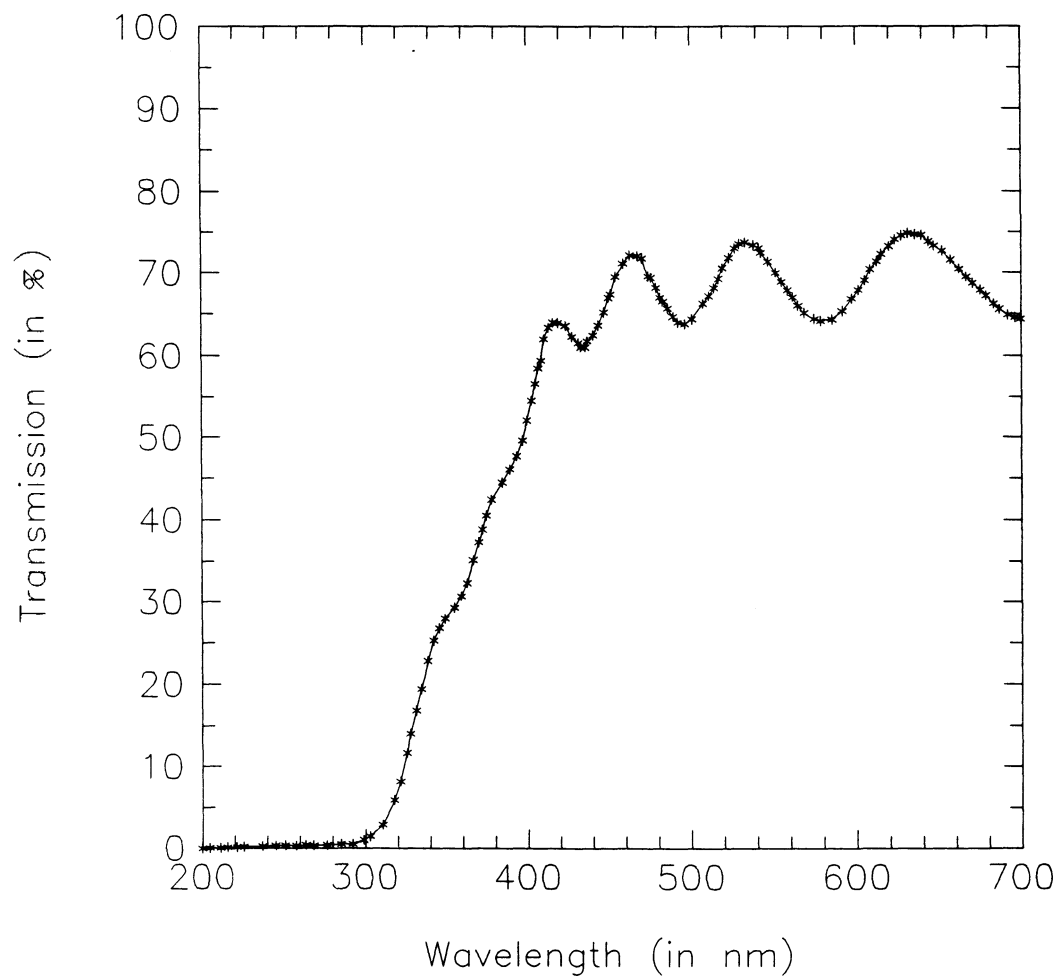


Figure 4.19a Transmission through the free standing polyimide film as a function of wavelength prior to irradiation.

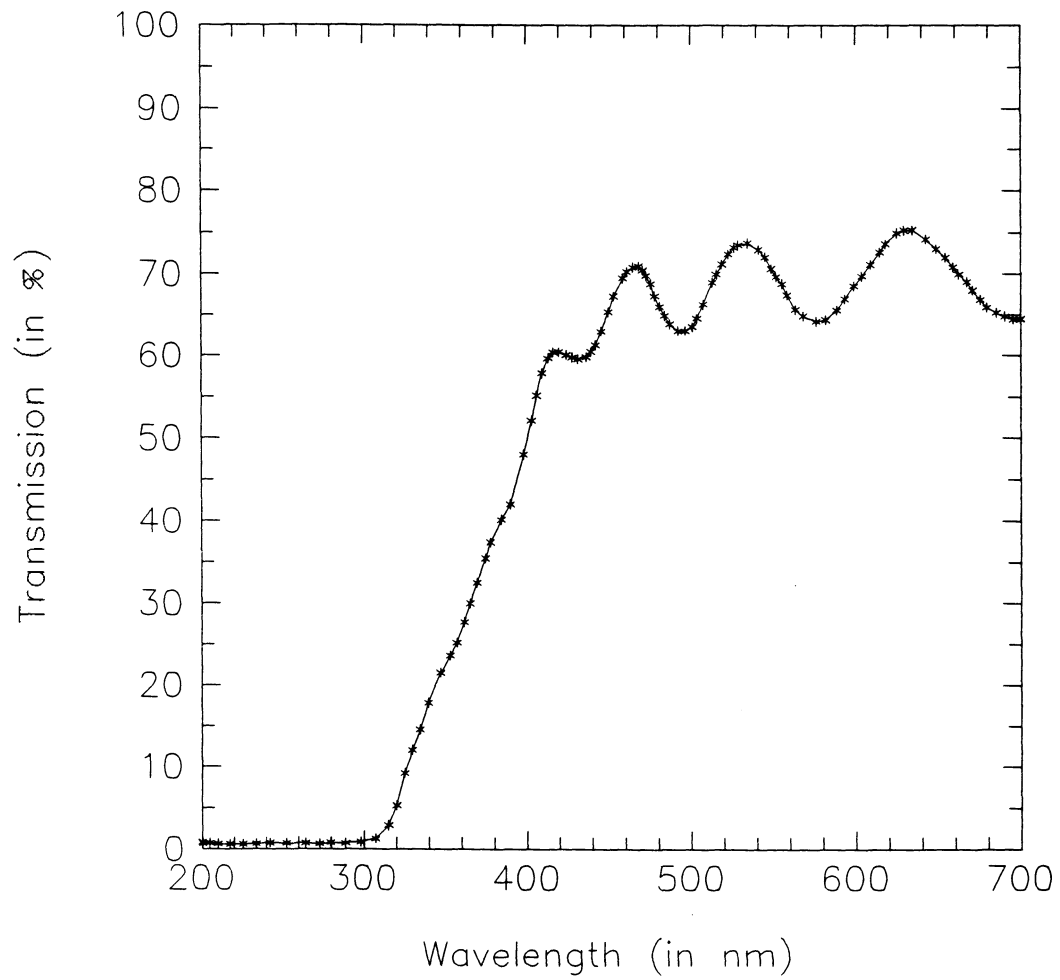


Figure 4.19b Transmission through the same film as a function of wavelength following irradiation.

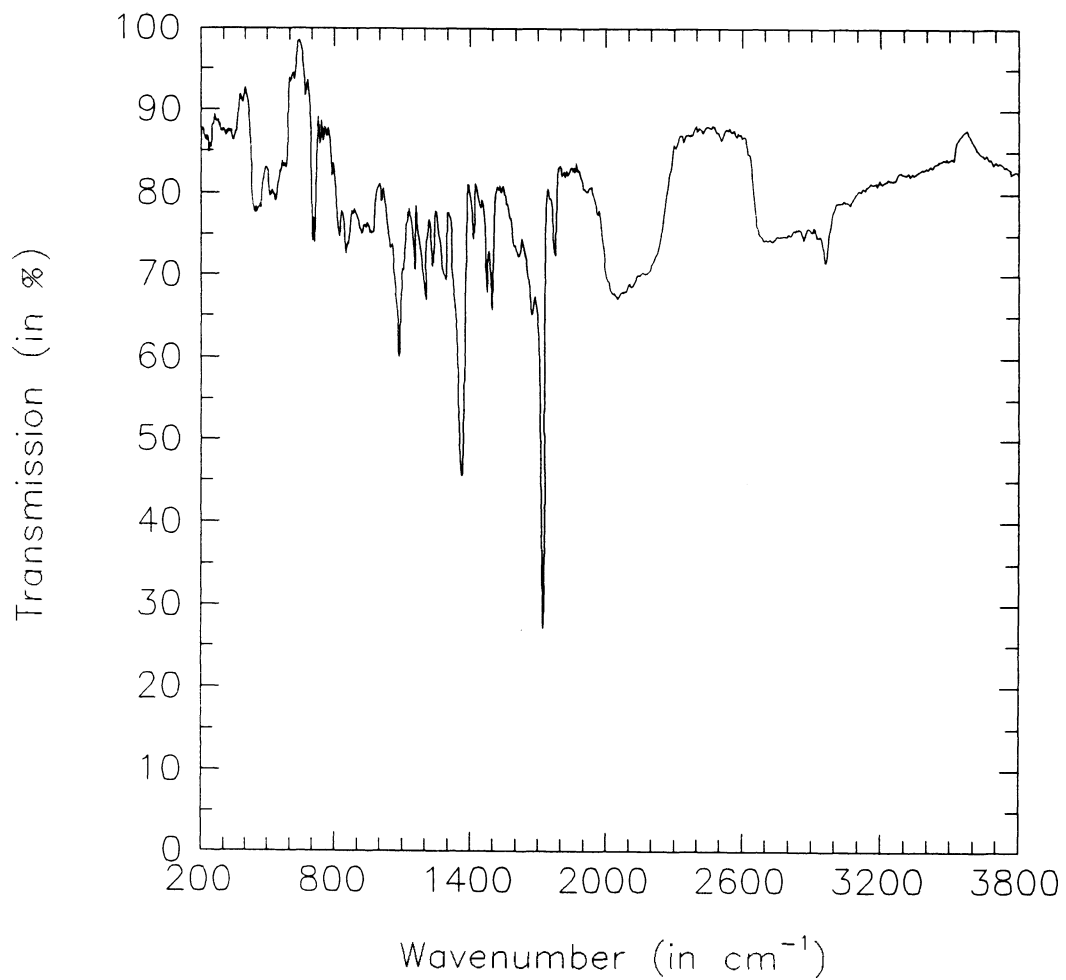


Figure 4.20a Infrared transmission of the film as a function of wavelength prior to irradiation.

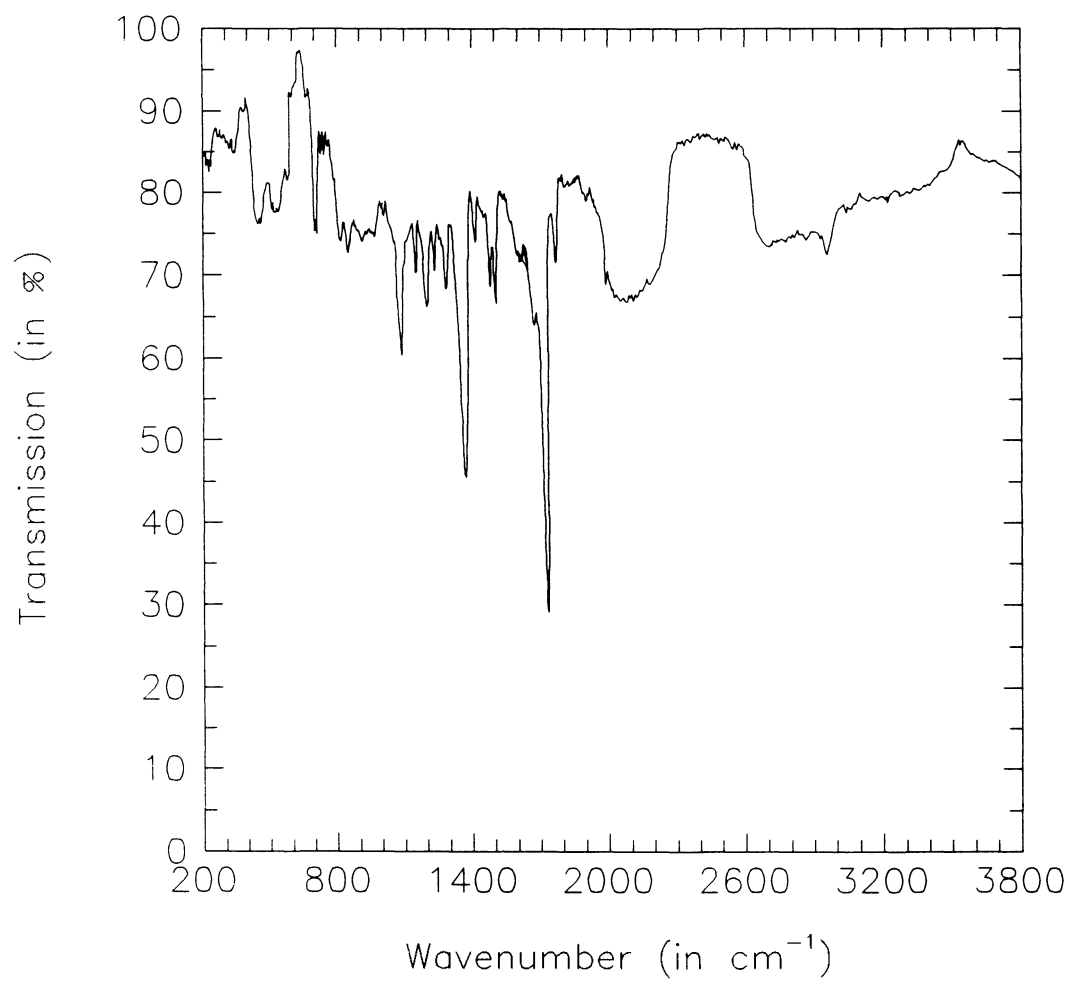


Figure 4.20b Infrared transmission of the same film following irradiation.

formation of new types of bonds did not take place. Although infrared spectroscopy indicated that low fluence pulses did not have an appreciable chemical effect on the film, there was a change in its physical appearance. Figure 4.21 is a photograph of the film following irradiation. The pattern of bright and dark lines is the result of wrinkles formed during irradiation. When the film was hit with a pulse, an audible "snap" was heard. This implied that the film underwent some physical stress when exposed to a pulse. Over hundreds of pulses the film eventually buckled and the wrinkles developed.

In our experiments, we did not find any evidence for the incubation of polyimide by 308 nm radiation. It is possible that incubation is a subtle effect which we were unable to detect. If this is the case, incubation would not play a significant role in the ablation process.

4.5 RESISTANCE MEASUREMENTS AS A DAMAGE INDICATOR

As mentioned earlier (see section 3.4.4), the objective of the resistance measurements was to detect microscopic damage before the onset of visible damage. Microscopic cracks which formed perpendicular to the length of the wire would decrease its cross-sectional area and increase its electrical resistance. Since the width of a single crack is small compared to the length of the wire (300 microns), its contribution to the total resistance is small and a sufficient number of cracks would have to form to obtain a measurable resistance change. Figure 4.22a is a SEM image of a 10 micron wide wire irradiated with 40 laser pulses at a fluence of 96 mJ/cm^2 per pulse. The first 20 pulses

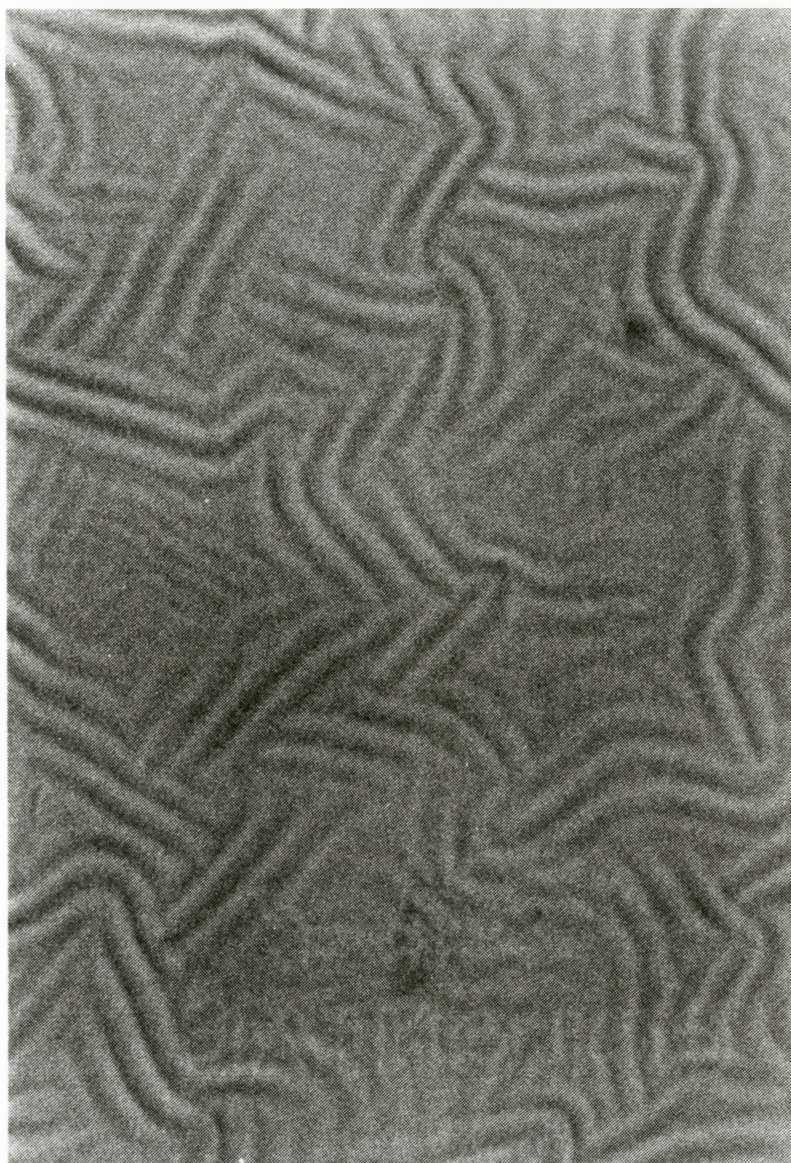


Figure 4.21 Photograph of the free standing film following irradiation.

gradually ablated the polyimide surrounding the wire, but there was no measurable change in the resistance of the wire itself. The next 20 incident pulses caused the surface of the aluminum to darken. This was most likely due to the formation of small cracks on the surface which caused the incident light to be scattered. It is also possible that the darkening was the result of redeposited polyimide. When the wire was hit with the fortieth pulse, its resistance suddenly increased to infinity, suggesting that the wire had been completely severed. This was confirmed when a relatively large crack was detected in the aluminum near the point where the wire meets the contact pad. The crack is shown in the right portion of Figure 4.22a. The section of aluminum immediately beside the crack was inadvertently moved while the sample was being prepared for SEM.

Figure 4.22b is a magnification of the previous photograph showing damage to a section of the wire. There are several cracks (approximately 4 to 5 microns long) which run perpendicular to the wire. There is also some damage along the edges of the wire. It is obvious from this figure that the underlying polyimide near the edge of the wire has taken on the same shape as the wire. In effect, the wire has acted as a mask, preventing the ablation of material in regions which it covers. Figure 4.22c is magnification of 4.22a, but of the section where the aluminum was inadvertently removed in preparation for SEM. The polyimide has been damaged in the same fashion as was seen in section 4.3.

At higher fluences, damage to the wire is expected to occur much sooner. Figure 4.23 is a SEM image of a 100 micron wide wire which was exposed to a single laser

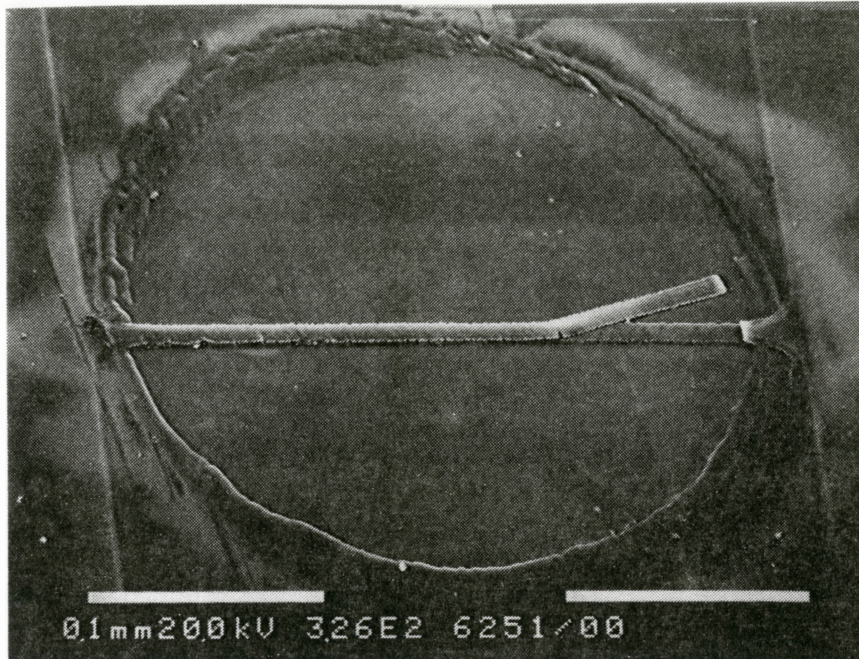


Figure 4.22a SEM image of a 10 micron wide wire irradiated with 40 laser pulses at a fluence of 96 mJ/cm^2 . The surrounding polyimide has been removed, leaving only the section under the wire.

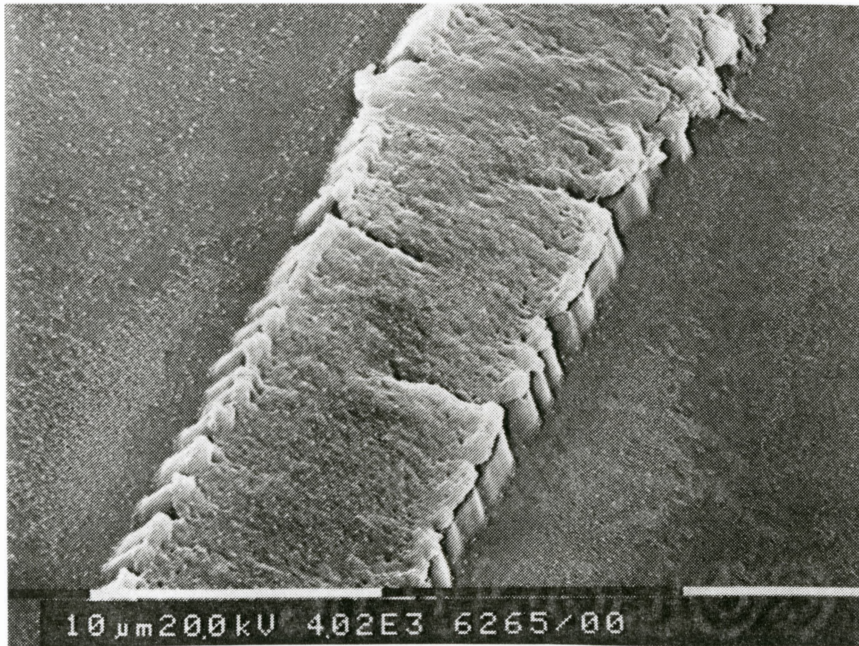


Figure 4.22b Magnification of Figure 4.22a, showing damage to a section of the aluminum wire.



Figure 4.22c Magnification of Figure 4.22a showing the region where the aluminum wire has inadvertently been lifted up in preparation for SEM, thereby revealing the underlying polyimide.

pulse at a fluence of 121 mJ/cm^2 . The fluence was large enough to cause cracking and lifting of the aluminum from the underlying polyimide. Although physical damage to the wire had occurred, its resistance was unchanged.

It is interesting to note that the fluences necessary to cause damage or removal of the aluminum wires is significantly less than for non-patterned aluminum films of the same thickness. This can be seen by comparing the results of this section to those in section 4.2. A possible reason for the discrepancy is that the required processing steps may have reduced the adhesion between the polyimide and the aluminum. Some blistering of the sample did occur while the photoresist was being removed. In addition, surface profiles of the patterned wires revealed that the surface was raised near the edges of the contact pads.



Figure 4.23 SEM image of a 100 micron wide wire exposed to a single laser pulse at a fluence of 121 mJ/cm^2 . The fluence was large enough to damage the wire.

5. CONCLUSIONS

The results for polyimide ablation are the following. As expected, the ablated depth varied linearly with the number of incident laser pulses. The presence of redeposited debris near the edges of the ablated holes was revealed by the surface profiles and confirmed by SEM. In addition, SEM showed that direct exposure of the underlying silicon substrate to incident pulses did not damage it. This was expected since the damage threshold for silicon is much larger than the ablation threshold for polyimide. When the ablation rate was examined as a function of the incident fluence, it was found that it could be successfully modelled by Equation 2.4. An ablation threshold of 67 ± 6 mJ/cm² was determined from Figure 4.5, which is in general agreement with previous results by other researchers. If the incident fluence is less than this threshold, the ablation rate is negligible. Fluences greater than the threshold value are required to achieve a significant rate of material removal.

Studies on the damage and removal characteristics of aluminum layers yielded favourable results. The damage thresholds were dependent upon the thickness of the aluminum layer, with thicker layers being more resilient to damage. The number of incident pulses was also important. In certain cases, damage would not appear until after exposure to hundreds of pulses. The damage threshold for sufficiently thin aluminum layers was less than the ablation threshold of polyimide. As a result, it was impossible to ablate polyimide without damaging the aluminum layer if both were exposed to the

same pulse. This was not true for thicker aluminum layers since their damage threshold was greater than the polyimide ablation threshold.

Removal of the aluminum layer was performed using a single shot removal technique. This technique produced holes which showed superior edge quality and did not result in the ablation of the underlying polyimide as did the multiple shot technique. The quality of the hole produced was also dependent upon the incident fluence. Splattering of molten aluminum near the edge of the hole occurred if an excessively large fluence was used. In addition, higher fluences resulted in damage to the underlying polyimide as well as in increased amounts of redeposited aluminum at the bottom of the hole. If the incident fluence was too low, the edges of the hole were not as sharp and only partial film removal occurred. Selection of the ideal fluence produced holes with superior edge quality, very little redeposited aluminum and no damage to the underlying polyimide.

Our results also showed that selective ablation of a polyimide-aluminum-polyimide multilayer was possible, depending on the thickness of the aluminum layer. If the aluminum layer was thin, it was difficult to remove the upper polyimide layer without damaging or removing the aluminum layer. For thicker aluminum layers, high fluences were required to produce good quality holes. As was the case for the holes ablated in the polyimide on silicon samples, there was once again redeposited debris around the edge of the hole.

Irradiation of the free standing polyimide films with low fluence laser pulses did

not produce any observable changes in the ultraviolet or infrared transmission spectra of the film. In order to affect the ablation rate, a significant portion of the film would have to be modified. Our results show that this was not the case, so it was concluded that incubation by 308 nm radiation is at best a subtle effect, and does not affect the ablation rate of polyimide. Although there appeared to be no chemical modification of the film, there was some physical damage. Exposure to hundreds of low fluence laser pulses eventually caused buckling and wrinkling of the film.

There were two primary conclusions drawn as a result of the resistance experiments. First, if resistance measurements are to be used as a quantitative method of characterizing physical damage to aluminum wires, a more sensitive technique to measure the resistance must be devised. Since the resistance remained constant or abruptly increased to infinity, it was impossible to smoothly correlate a resistance change to the induced damage. Second, there was often little or no change in the resistance over a series of laser pulses, although it was evident that physical damage was occurring. These results indicate that a small amount of laser induced damage may be tolerated. However, such physical damage may ultimately affect the durability and reliability of such a wire and should therefore be minimized.

There are several directions in which future work could proceed now that it has been shown that ablation works quite well as a material removal technique. Since the laser operates at a short wavelength, it would be interesting to determine the minimum feature size which could be produced using this technique. It would also be interesting

to pattern features such as wires, contact pads, *etc.*, in the layers and compare the quality of this technique with other ones. Since ablation often resulted in redeposited debris surrounding the hole, methods to reduce this debris should be explored. One possible way to accomplish this would involve performing the ablation in a vacuum.

6. APPENDICES

APPENDIX A: Graphs of the ablated depth versus the number incident pulses for polyimide at various laser fluences.

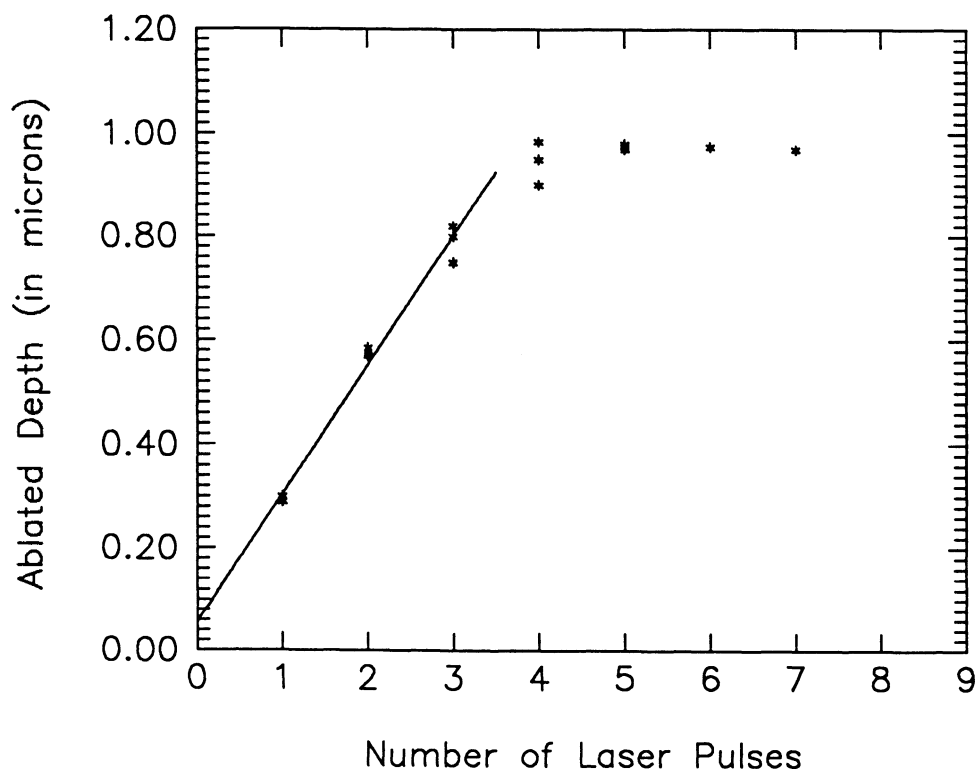


Figure A.1 Ablation performed at an incident fluence of 470 mJ/cm².

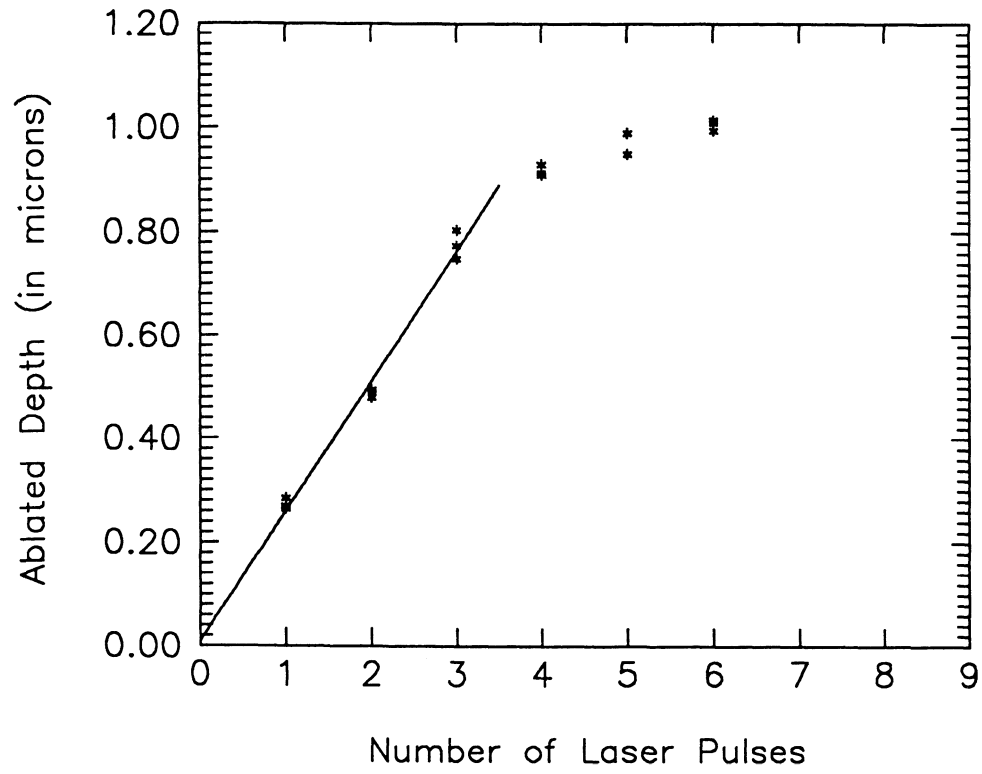


Figure A.2 Ablation performed at an incident fluence of 373 mJ/cm^2 .

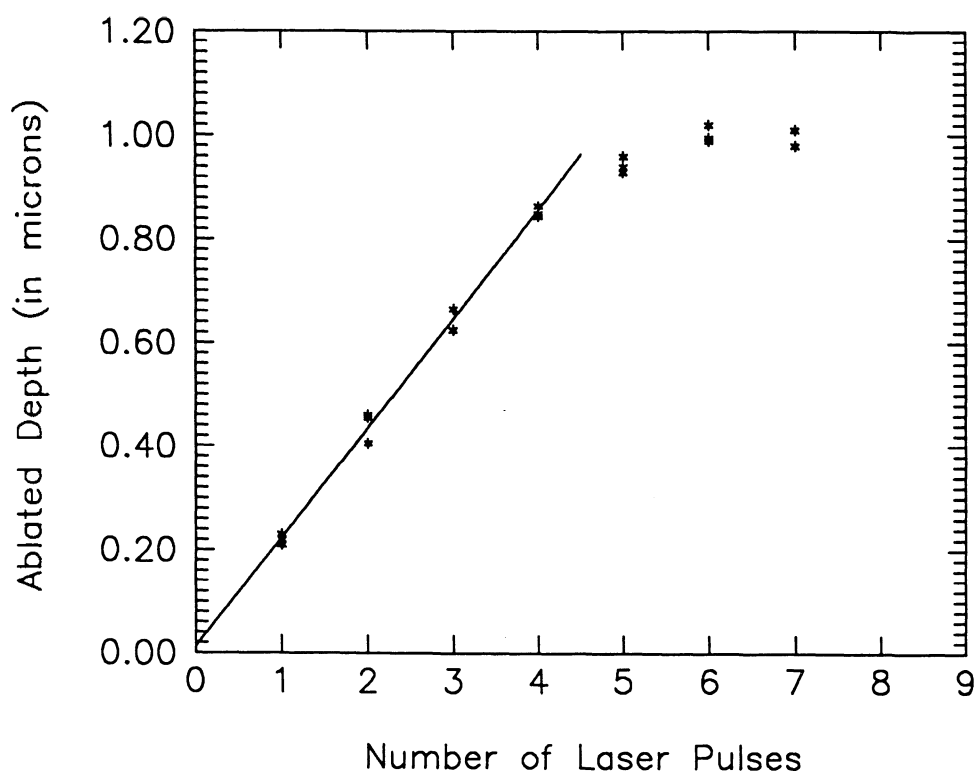


Figure A.3 Ablation performed at an incident fluence of 297 mJ/cm^2 .

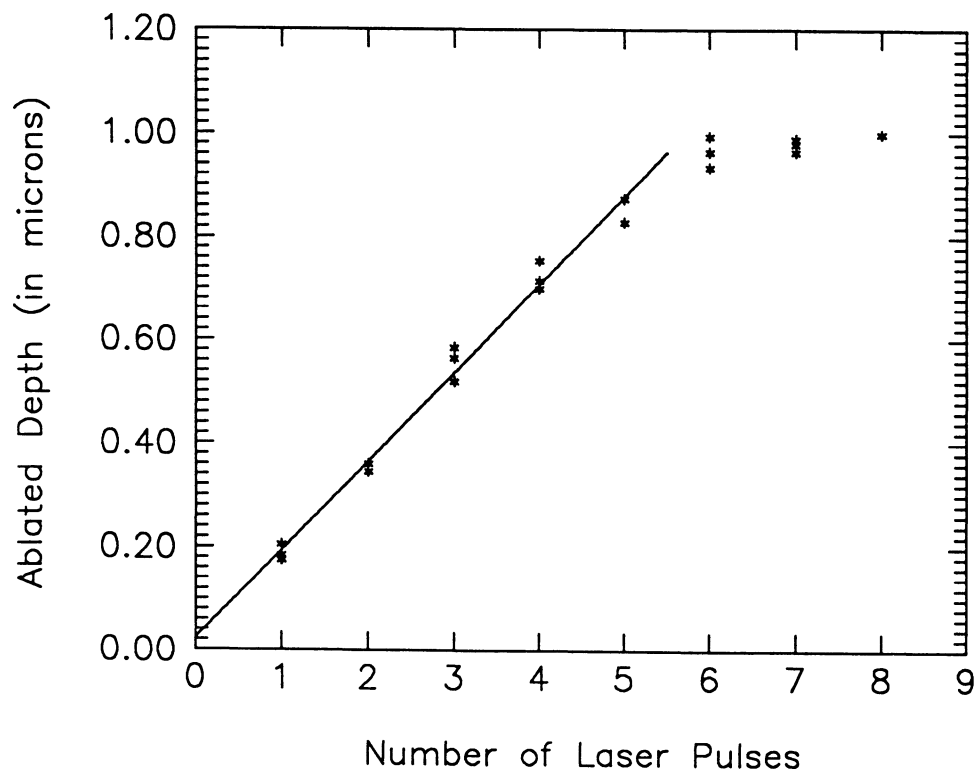


Figure A.4 Ablation performed at an incident fluence of 236 mJ/cm².

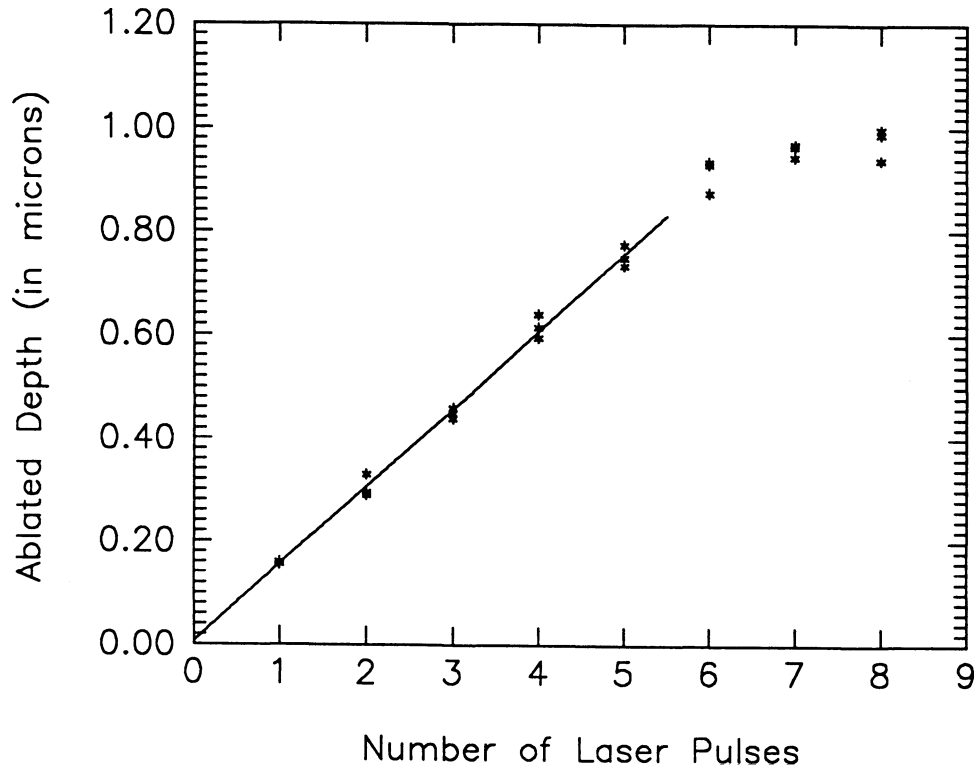


Figure A.5 Ablation performed at an incident fluence of 187 mJ/cm^2 .

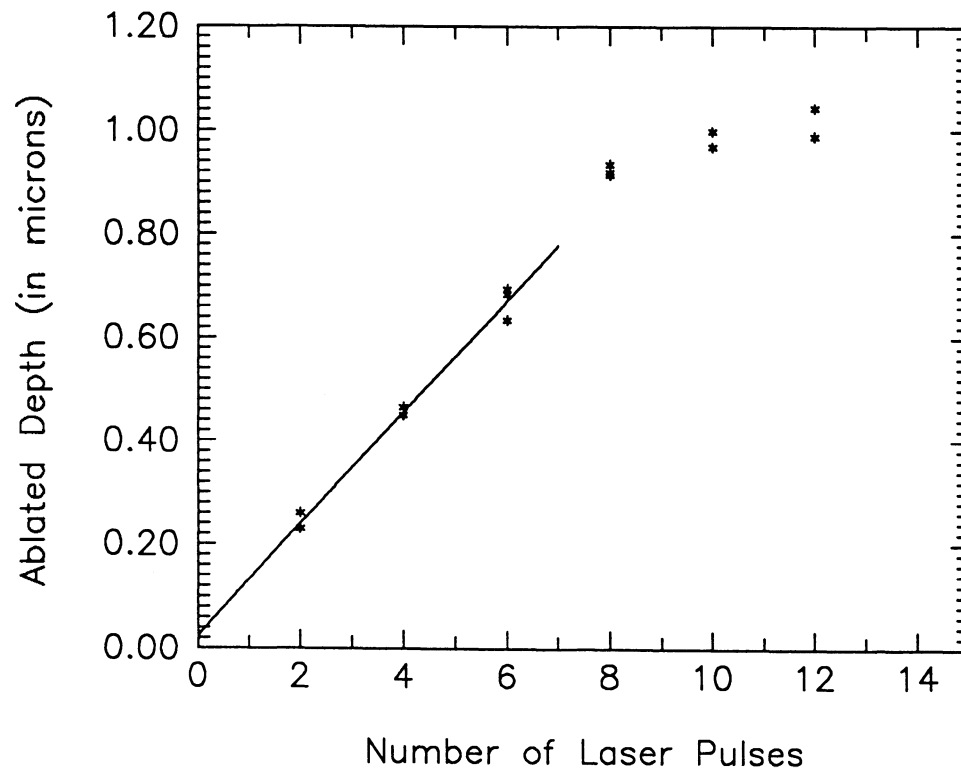


Figure A.6 Ablation performed at an incident fluence of 149 mJ/cm^2 .

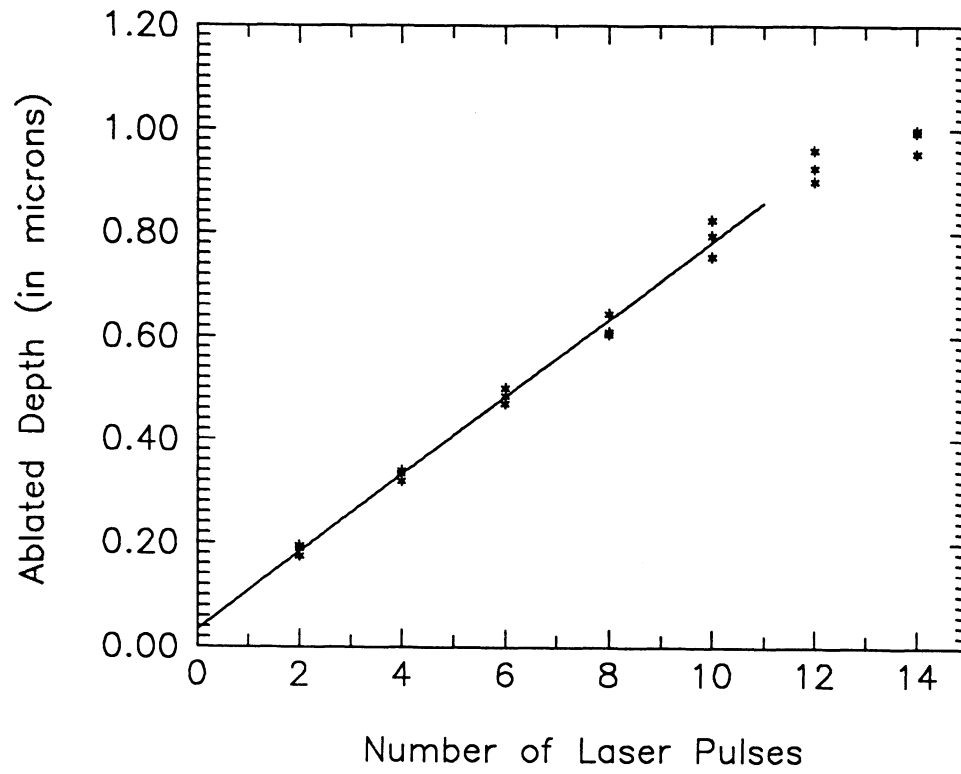


Figure A.7 Ablation performed at an incident fluence of 118 mJ/cm^2 .

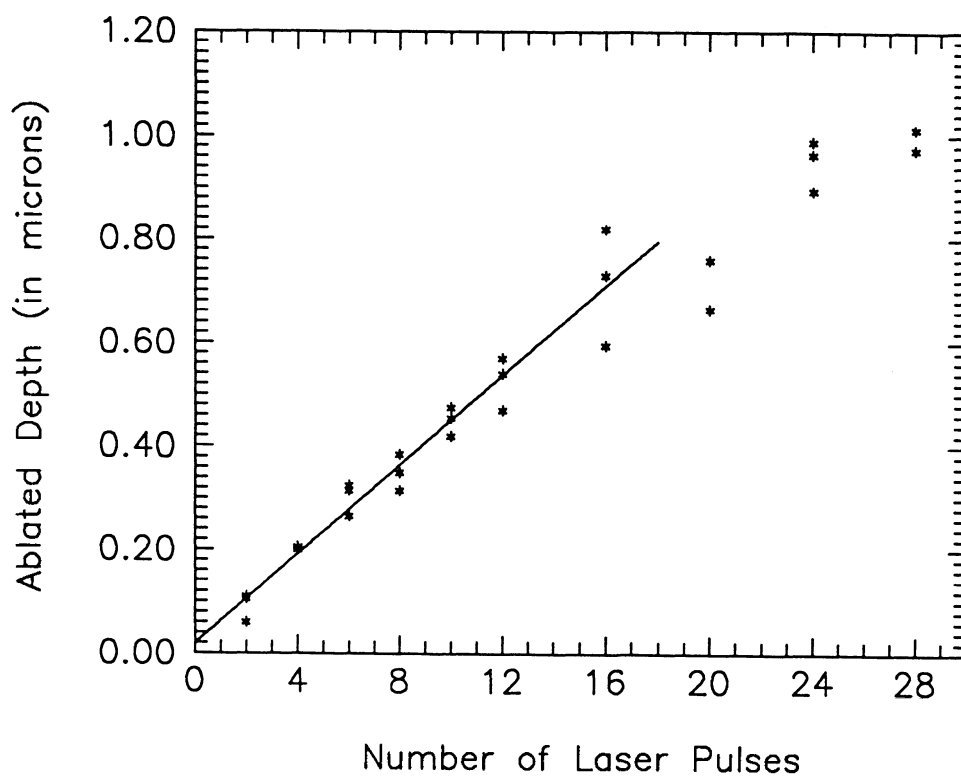


Figure A.8 Ablation performed at an incident fluence of 94 mJ/cm².

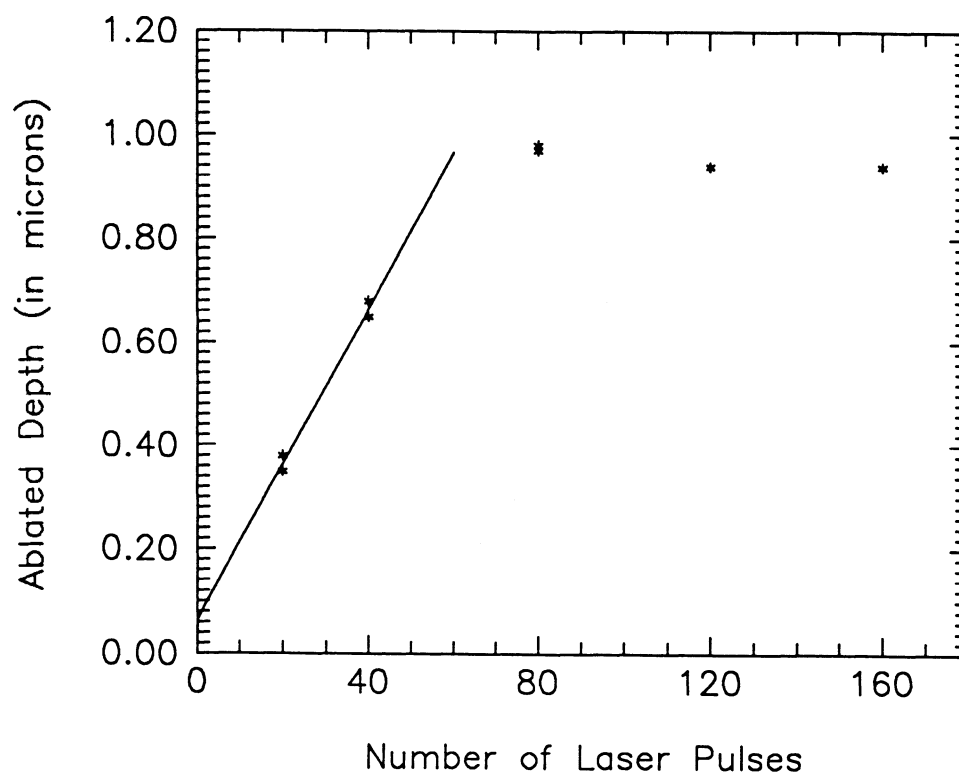


Figure A.9 Ablation performed at an incident fluence of 74 mJ/cm^2 .

APPENDIX B: Calculation of the temperature rise in the irradiated section of an aluminum layer by a single incident laser pulse.

The expression for the temperature rise in the irradiated area is given below; where F is the incident fluence (in J/cm^2), A is the size of the irradiated area (in cm^2), R is the reflectivity of aluminum at 308 nm, ρ is the density of aluminum, C_p is the specific heat capacity of aluminum, t is the film thickness (in cm) and ΔT is the temperature rise in the film.

$$\begin{aligned}\Delta T &= \frac{\Delta \text{Energy}}{\text{mass } C_p} \\ &= \frac{F A (1-R)}{\rho V C_p} \\ &= \frac{F A (1-R)}{\rho A t C_p} \\ \therefore \Delta T &= \frac{F (1-R)}{\rho C_p t}\end{aligned}$$

Given that $R = 0.925$,²⁰ $\rho = 2.70 \text{ g/cm}^3$,²⁸ $C_p = 0.866 \text{ J/g } ^\circ\text{C}$,²⁸ $t = 235 \text{ nm} = 2.35 \times 10^{-5} \text{ cm}$ (for this particular layer) and assuming an incident fluence of 650 mJ/cm^2 (0.65 J/cm^2), the temperature rise in the film is approximately 890°C . If the incident fluence is lowered to 326 mJ/cm^2 , then the temperature rise is only about 445°C . This

calculation assumes that heat loss due to diffusion is negligible. Since the heat will only diffuse about 2.8 microns on the timescale of the incident pulse (see section 2.1.1) and the irradiated area is much larger than this distance, our assumption is valid.

7. REFERENCES

- 1 P.E. Dyer and J. Sidhu. "Excimer laser ablation and thermal coupling efficiency to polymer films" *J. Appl. Phys.* **57**(4), (1984) p. 1420
- 2 M. Latta, R. Moore, S. Rice and K. Jain. "Excimer laser projection photoetching" *J. Appl. Phys.* **56**(2), (1984) p. 586
- 3 J.E. Andrew, P.E. Dyer, D. Forster, and P.H. Key. "Direct etching of polymeric materials using a XeCl laser" *Appl. Phys. Lett.* **43**(8), (1983) p. 717
- 4 R. Srinivasan and V. Mayne-Banton. "Self-developing photoetching of poly(ethylene terephthalate) films by far-ultraviolet excimer laser radiation" *Appl. Phys. Lett.* **41**(6), (1982) p. 576
- 5 R. Srinivasan, E. Sutcliffe and B. Braren. "Ablation and etching of polymethylmethacrylate by very short (160 fs) ultraviolet (308 nm) laser pulses" *Appl. Phys. Lett.* **51**(16), (1987) p. 1285
- 6 J.H. Brannon, J.R. Lankard, A.I. Baise, F. Burns and J. Kaufman. "Excimer laser etching of polyimide" *J. Appl. Phys.* **58**(5), (1985) p. 2036
- 7 R. Srinivasan, B. Braren and R.W. Dreyfus. "Ultraviolet laser ablation of polyimide films" *J. Appl. Phys.* **61**(1), (1987) p. 372
- 8 V. Srinivasan, M.A. Smrtic and S.V. Babu. "Excimer laser etching of polymers" *J. Appl. Phys.* **59**(11), (1986) p. 3861

- 9 G.M. Davis, D.W. Thomas, and M.C. Gower. "Excimer laser direct etching of GaAs" *J. Phys. D: Appl. Phys.* **21**, (1988) p. 683
- 10 G.B. Shinn, F. Steigerwald, H. Stiegler, R. Sauerbrey, F.K. Tittel and W.L. Wilson Jr. "Excimer laser photoablation of silicon" *J. Vac. Sci. Technol. B* **4(6)**, (1986) p. 1273
- 11 J.G. Black, D.J. Ehrlich, M. Rothschild, S.P. Doran and J.H.C. Sedlacek. "Laser-direct-writing processes: Metal deposition, etching, and applications to microcircuits" *J. Vac. Sci. Technol. B* **5(1)**, (1987) p. 419
- 12 F. Bachmann. "Excimer lasers in a fabrication line for a highly integrated printed circuit board" *Chemtronics* **4(3)**, (1989) p. 149
- 13 K.J. Polasko, D.J. Elliott and B.P. Piwczyk. "Very large scale integrated pattern registration improvement by photoablation of resist-covered alignment targets" *J. Vac. Sci. Technol. B* **6(1)**, (1988) p. 389
- 14 D.E. Seeger and M.G. Rosenfield. "Clearing resist from alignment mark areas using an excimer laser" *J. Vac. Sci. Technol. B* **6(1)**, (1988) p. 399
- 15 J.E. Andrew, P.E. Dyer, R.D. Greenough and P.H. Key. "Metal film removal and patterning using a XeCl laser" *Appl. Phys. Lett.* **43(11)**, (1983) p. 1076
- 16 J.G. Black, S.P. Doran, M. Rothschild and D.J. Ehrlich. "Supplemental multilevel interconnects by laser direct writing: Application to GaAs digital integrated circuits" *Appl. Phys. Lett.* **50(15)**, (1987) p. 1016

- 17 M. Rothschild and D.J. Ehrlich "A review of excimer laser projection lithography" J. Vac. Sci. Technol. B **6**(1), (1988) p. 1
- 18 D.L. Singleton, G. Paraskevopoulos, A.D. Buckthought, R.S. Irwin, G.S. Jolly and I.T. Ali Emesh. "Investigation of photoablation as a patterning technique for silicon based integrated circuits: laser ablation and physical damage threshold considerations" Proc. SPIE, vol. 1186, Surface and Interface Analysis of Microelectronics Materials Processing and Growth, (1989)
- 19 Rolf E. Hummel. Electronic Properties of Materials: An Introduction for Engineers, Springer-Verlag, New York, (1985) p. 142
- 20 CRC Handbook of Chemistry and Physics, 72nd edition, CRC Press, Boston, (1991-92) p. 12-101
- 21 R. Srinivasan. "Ablation of Polymers and Biological Tissue by Ultraviolet Lasers" Science **234**, (1986) p. 559
- 22 E.E.B. Campbell, G. Ulmer, K. Bues and I.V. Hertel. "Analysis of Ionic Fragments from 308 nm Photoablation of Polyimide" Appl. Phys. A **48**, (1989) p. 543
- 23 S. Kuper and M. Stuke. UV-Excimer-Laser Ablation of Polymethylmethacrylate at 248 nm: Characterization of Incubation Sites with Fourier Transform IR- and UV- Spectroscopy" Appl. Phys. A **49** p. 211
- 24 P. Heszler, Zs. Bor and G. Hajos. "Incubation Process in Polyimide upon UV Photoablation" Appl. Phys. A **49**, (1989) p. 739

- 25 S. Lazare, V. Granier, P. Lutgen and Y. Novis. "Selectivity in UV laser metal ablation of aluminized Mylar" *Chemtronics* **4**(3), (1989) p. 159
- 26 CRC Handbook of Chemistry and Physics, 72nd edition, CRC Press, Boston, (1991-92) p. 4-36
- 27 R. Srinivasan and B. Braren. "Ablative Photodecomposition of Polymer Films by Pulsed Far-Ultraviolet (193 nm) Laser Radiation: Dependence of Etch Depth on Experimental Conditions" *Journal of Polymer Science* **22**, (1984) p. 2601
- 28 CRC Handbook of Chemistry and Physics, 72nd edition, CRC Press, Boston, (1991-92) p. 12-119